POLITECNICO DI TORINO

Master's Degree in Civil Engineering

Master's Degree Thesis

Nonlinear and scaling effects on creep crack propagation

Supervisor

Prof. Alberto Carpinteri

Co-Supervisor

Dr. Gianni Niccolini

Candidate

Alessio Rubino

October 2018

CONTENTS

ACKNOWLEDGEMENTS

I would like to express my gratitude to my supervisors, Professor Alberto Carpinteri and Doctor Gianni Niccolini, for their continued support during these last months.

PERSONALI

Questo intero percorso, durato ben sette anni, lo dedico alla mia famiglia. Ai miei genitori e ai mie fratelli, sempre presenti. Durante questo lungo, e duro, periodo abbiamo dovuto affrontare sfide significative. E' stato necessario dare il meglio di noi, per superare difficoltà fino a quel momento inesplorate. L'importante è essere arrivati qui, uniti. Come vedete, il senso di tutto ciò viene compreso solo alla fine, dopo enormi sacrifici, e non poteva essere più bello di così.

Ai miei zii e cugini "torinesi", grazie per avermi fatto sentire a casa.

A mio nonno Giuseppe, grazie per l'esempio.

Ai miei amici di una vita, grazie. Ho sentito il vostro supporto anche a distanza.

Ai miei compagni di viaggio, Nicola, Virginia e Martina. Siete stati linfa quotidiana durante questa esperienza. Sarete sempre con me, ovunque.

A Felice, grazie per avermi sopportato.

Ai miei colleghi tutti, grazie per essere stati accanto a me.

All' Ing. Luigi Gentile, grazie per avermi indicato la strada.

ABSTRACT

Several structural components of power plants, chemical reactors and turbines are subjected to relevant stress states and high temperatures. These particular conditions, i.e. creep conditions, have to be accounted for the design of these high-temperature components. Under these circumstances, an assessment of time-dependent creep deformations is needed. It may happen that, at the end of the predicted creep rupture life, a crack nucleates at a high-stress site and propagates until failure occurs. Considering that the "flaw-free" condition is only a theoretical assumption, failure is most likely due to the propagation of a pre-existing defect. In this case, the entire life of the component is spent in crack propagation. For this reason, it is important to achieve an accurate knowledge about the crack growth under creep conditions, in order to provide a prediction of the creep life.

This work is organized to comprehensively deal with the fundamental aspects of creep behaviour, regarding materials operating under the above described conditions. After a general introduction of the phenomenon, the first part provides an overview of the experimental work reported in literature. In particular, the influence of several parameters on the creep crack growth rate (CCGR) are extensively analysed.

The second part deals with scaling effects governing creep, both for smooth and notched specimens, by analogy with fatigue phenomenon. Particular attention will be paid on the specimen size effect on creep rupture time, and on the crack size effect on CCGR. Although a voluminous scientific literature can be found regarding the creep phenomenon, only a few research works focused on such

scaling effects. In this work, these effects will be approached by means of the dimensional analysis, where the emerging self-similarity will be interpreted also in the framework of fractal geometry. These findings are enriched by considering the material nonlinearity.

1.REVIEW OF PREVIOUS EXPERIMENTAL WORKS

1.1 Introduction

An extensive description of the life of engineering components subjected to creep conditions is provided. In the past years, researchers deal with the problem of creep life prediction following two basic approaches. The first approach is more traditional and applies to unnotched, nominally flaw-free, specimens to determine the time to failure, related to imposed values of stress and temperature. In this context, creep life predictions can be carried out at fixed temperature and geometry, by plotting experimental data of applied stress vs time to rupture.

A more recent approach, based on time-dependent fracture mechanics (TDFM), has been developed to characterize the creep crack growth rate, da/dt, as a function of a controlling parameter, which is to be determined. In this case, creep life assessment can be obtained by evaluating the growth of a pre-existing crack, until its "critical" value causing material fracture is reached. As the first approach is more easily applicable for life prediction purposes, it has received more attention. Conversely, the second approach is more refined and allows more accurate predictions, though it can be troublesome at the early stages of crack growth. A review of the existing experimental work based on these approaches is provided in this chapter.

In the second section a description of creep behaviour for smooth specimen is provided, assuming "flaw-free" condition. On the other hand, in the third section the applicability of Fracture Mechanics concepts for predicting creep crack growth

rate (CCGR) in notched specimens is discussed in the framework of TDFM. It will be highlighted how useful are the analogies between TDFM and Elastic-plastic fracture mechanics (EPFM) to extend the fracture mechanics concepts to conditions of time-dependent creep deformations. A wide range of experimental works is considered. In the concluding section Q^* parameter, more recently proposed in literature, is presented. Assuming that creep crack growth is a thermally activated process, this parameter has been derived by the analysis of numerous experimental tests.

1.2 Creep behaviour of smooth specimens

Creep (sometimes called cold flow or fluage) is the tendency of solid materials to deform slowly and permanently under the action of mechanical loads. More precisely, a material is said to creep when time-dependent deformations are observed as a result of long-term exposure to relatively high constant stress levels that are still below the yield strength of the material. The creep phenomenon occurs when the temperature is relatively high, falling in a range which depends on the material. It is found that creep effects start to be noticeable at about 40% of the absolute melting temperature of material. The ratio between actual and absolute melting temperatures of the tested material is also called "homologous" temperature.

It is possible to grasp the main features of the phenomenon by the simple observation of a typical creep curve. This curve, shown schematically in fig. 1.1, represents the relationship between creep deformation and time.

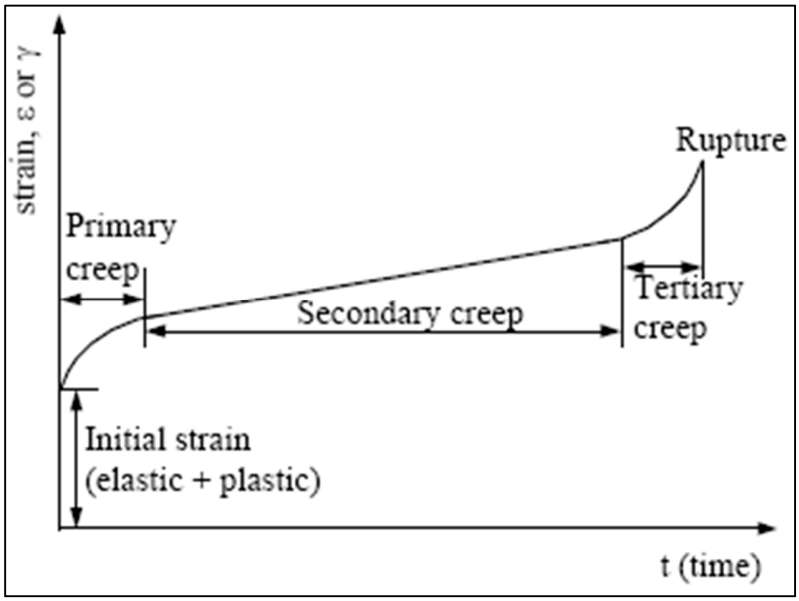

Figure 1.1 – Typical creep curve

Looking at the curve, it seems convenient to separate it into three stages, o regions. After an instantaneous deformation, due to elastic and plastic contributions, primary creep occurs. As creep proceeds during the test, the strain rate decreases with time to a minimum, and becomes near constant as the secondary stage starts. The secondary stage, or "steady-state creep", is characterized by a constant value of strain rate. Finally, in the "tertiary creep region", strain rate accelerates until material fracture occurs.

For several materials primary creep is short-lived or doesn't exist at all. Furthermore, tertiary creep regime is not attractive for design purposes, because it must be avoided. These remarks make the steady-state region the most important for design purposes, also because the largest part of the creep life is spent in this stage. For this reason, later discussion will be focused on the steady-state region.

Creep behaviour is strongly dependent on several factors, such applied stress, temperature, specimen size. Generally, we can say that an increase of temperature makes creep more severe, raising the level of the creep curve. In this section, only the stress influence on minimum strain rate (which refers to the constant rate in the secondary stage) and on time rupture will be analysed in detail. Other dependencies will be pointed out later, in the second chapter of this work.

(A)Stress dependence of steady-state strain rate

Stress dependence of steady-state strain rate can be evaluated by carrying out the so called "creep test", which is conceptually quite simple. A constant load is applied to the test specimen maintained at a constant high temperature. Measurements of strain are then recorded over the time until failure occurs. As a basic result, the "creep curve" shown in fig. 1.1 is obtained. The creep test is usually focused on determining the minimum value of the strain rate, i.e. steady-state strain rate, related to the applied stress at the specific temperature. Repeating this procedure for a certain stress range, a relationship between applied stress and minimum strain rate at fixed temperature can be found. Data of such deformation are needed by engineers for design purposes. As expected, it is found that the minimum strain rate increases with increasing applied stress.

Reports of experimental results published in Garofalo [8], propose several empirical expressions for the steady-state strain rate $\dot{\varepsilon}_s$ as a function of the applied stress σ. Data plots are shown in fig. 1.2

At low stress levels, the best fit of experimental data is provided by the following correlation, also known as Norton's law:

$$\dot{\varepsilon}_s = A\sigma^n \tag{1.1}$$

represented by a straight line in a log-log graph.

At high stress levels, deviations from linearity are observed, and a better correlation is provided by the following equation:

$$\dot{\varepsilon}_s = A' \exp(\beta\sigma) \tag{1.2}$$

Both behaviours can be described by a unique relationship as follows:

$$\dot{\varepsilon}_s = A''(\sinh \alpha\sigma)^n \tag{1.3}$$

It can be shown that the expression in Eq. (1.3) reduces to Eq. (1.1) for small values of $\alpha\sigma$ and to that in Eq. (1.2) for high values of $\alpha\sigma$, respectively. The fitting parameters *A''*, α and *n* depend on the applied temperature.

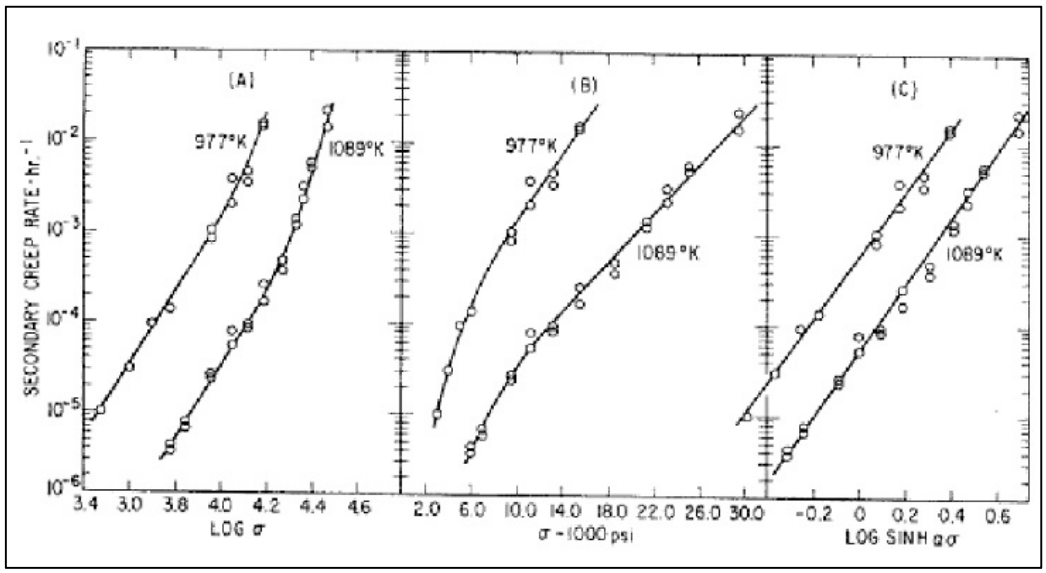

Figure 1.2 – Norton's law reported in [15]

(B) Stress dependence of rupture time

Stress dependence of the rupture time can be found out by carrying out the so called “stress rupture test”. This test is practically the same as the creep test, aside from the higher stress levels used, but it is focused on determining the rupture time. Experimental results for austenitic stainless steel, show a decrease of rupture time when higher stress is applied (fig 1.3).

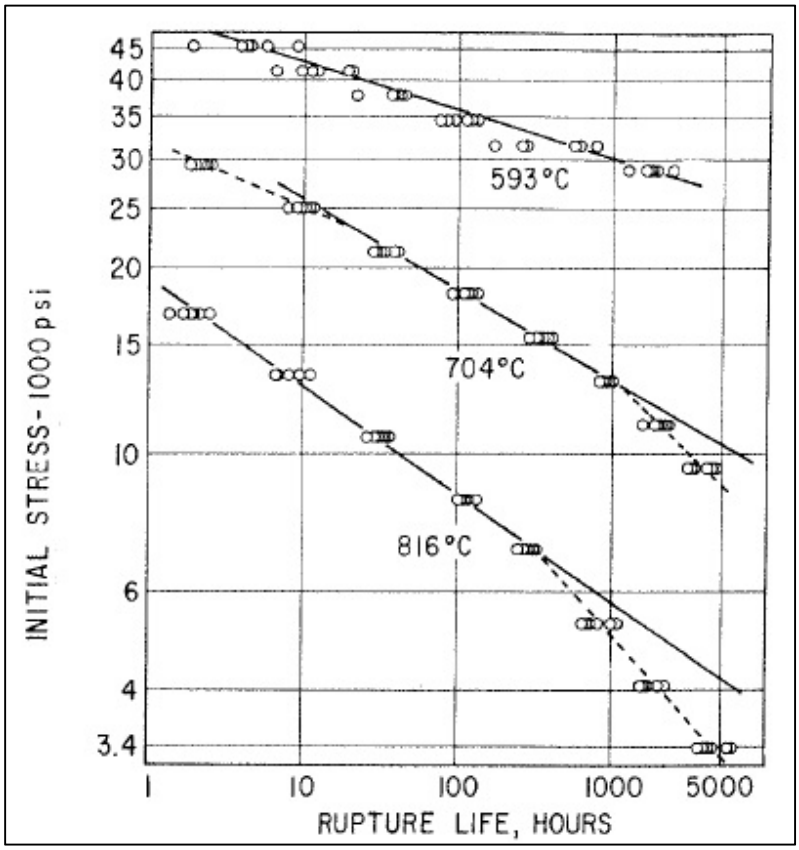

Figure 1.3 - Creep rupture diagrams reported in [15]

Several empirical formulae have been proposed in literature to correlate the applied stress and the rupture time. Among all of them, the most mentioned in the scientific literature is probably a power-law relationship:

$$t_R = B\sigma^{-P} \tag{1.4}$$

where t_R is the time to rupture, σ is the applied stress, B and p are material constants. Accordingly to Eq. (1.4), power-law trends are shown in the log-log diagram of Fig. 1.3 at different temperatures of interest.

The discussion about creep presents considerable analogies with the fatigue phenomenon. In both cases an increase of the applied stress results in a reduction of the life component. From an analytical point of view, the analogy emerges comparing Eq. (1.4) with Eq. (1.5), the Basquin law for fatigue [1]:

$$N \simeq \left(\frac{\Delta\sigma_y}{\Delta\sigma}\right)^n = (1-R)^n {\Delta\sigma_y}^n \Delta\sigma^{-n} \tag{1.5}$$

It is worth saying that while the fatigue life is represented by the number of cycles to failure, i.e. by the Wöhler's curve, creep life is described by the rupture time. In conclusion, in both cases a power-law relationship between the applied stress and the corresponding parameter representing the life component is established.

1.3 Creep crack growth: A fracture mechanics approach

With the advent of fracture mechanics, a more ambitious task was undertaken, which is understanding the propagation of cracks or flaws in components operating in creep conditions. Since the early 70's, numerous researchers contributed immensely to develop approaches and experimental techniques to describe the creep deformation kinetics in terms of creep crack growth rate (CCGR). At the beginning, several studies focused on finding the appropriate fracture mechanics parameter able to characterize CCGR. More precisely, numerous researchers argued that CCGR was controlled by the elastic stress intensity factor *K* or by some form of net-section stress.

Already in 1970, Siverns and Price [33] published experimental results, regarding crack growth under creep conditions. In that case, tests were carried out on 2.25%Cr 1%Mo steel at the temperature of 565 °C. Edge-notched rectangular cross-section specimens were tested under constant tensile stress, at several stress values of interest. Crack length was measured by using the electrical resistance method. It was found that all the results obey a relation of the following form:

$$\frac{\mathrm{d}a}{\mathrm{d}t} = C_0 \, K^m \tag{1.6}$$

where d*a*/d*t* is the crack growth rate, *K* is the elastic stress-intensity factor, C_0 and *m* are material constants. It was found that *m* was very close to the stress sensitivity of creep *n* in the Norton's law of Eq. (1.1), relating the minimum strain rate to the applied stress. Correlation between crack growth rate and net section stress was also attempted, yielding as a result a bundle of approximately parallel

lines, different for each test. In conclusion, results tended to designate the stress intensity factor as the best correlating parameter, as confirmed later by the same authors in another research work [34]. It must be noticed that eq. (1.6) seems to be the creep analogous of the Paris law defined for fatigue.

In the same period, other authors observed different trends about the prediction of creep crack growth rate. For instance, Harrison and Sandor [18] discussed the results obtained by The General Electric Turbine Department, testing centre-notched plate specimens at 1000 F. A correlation of the data was attempted both with stress intensity factor and net section stress. Although the correlation with K seemed reasonable, when all data points were plotted vs net section stress they fell into a very narrow band. Creep crack growth rate was described by the equation:

$$\frac{\mathrm{d}a}{\mathrm{d}t} = N\sigma_N{}^q \tag{1.7}$$

where da/dt is the crack growth rate, σ_N is the net section stress, N and q are material constants. A similar result was achieved by Nicholson and Formby ([23], [24]). In this case authors carried out creep rupture tests on single edge notched and notched centre hole specimens of solution treated A.I.S.I. type 316 stainless steel. Tests were performed at 740 °C. When CCGR was plotted against stress intensity factor, different curves were obtained for each specimen geometry considered. Conversely, when net section stress was used all the data fell on one curve, regardless of the specimen geometry tested. In conclusion, these experimental works supported the observation that the net section stress is a successful parameter for CCGR prediction.

Forward in time, other authors [22] followed this kind of approach, making a comparison between the suitability of these two parameters. But a unifying approach, was still not defined.

When substantial creep deformation accompanies fracture, it is expected that nonlinear fracture mechanics should be more relevant than linear elastic fracture mechanics. For this reason, a basic background regarding nonlinear fracture mechanics is now recalled. Later, we will try to extend the concepts of fracture mechanics to cracks under creep conditions.

The nonlinear behaviour of elastic-plastic materials with power-law hardening can be represented by the following relationship between stress and strain, in the form proposed by Ramberg and Osgood:

$$\varepsilon = \varepsilon_{el} + \varepsilon_p = \frac{\sigma}{E} + \alpha\varepsilon_0 \left(\frac{\sigma}{\sigma_0}\right)^n \tag{1.8}$$

where ε is the total strain, ε_{el} is the elastic strain, ε_p is the plastic strain, E is the Young's modulus, σ_0 is the yield strength, $\varepsilon_0 = \sigma_0/E$, α and n are regression coefficients. Particularly, n is the strain hardening exponent.

Rice [28] defined the following line integral, called J-integral, as a parameter to characterize nonlinear elastic materials ahead a crack:

$$J = \int_\Gamma W \, \mathrm{dy} - T_\mathrm{i} \left(\frac{\partial u_\mathrm{i}}{\partial \mathrm{y}}\right) \mathrm{ds} \tag{1.9}$$

where:

$$W = \int_0^{\varepsilon_{\mathrm{ij}}} \sigma_{\mathrm{ij}} \, \mathrm{d}\varepsilon_{\mathrm{ij}} \tag{1.10}$$

W is the strain-energy density associated with the point stress σ_{ij} and strain ε_{ij}, T_i is the traction vector defined by the outward normal n_j along an arbitrary contour Γ surrounding the crack tip: the integral is evaluated in a counterclockwise sense from the lower crack surface and continuing along the path Γ to the upper crack surface as shown in Fig. 1.4.

The utility of the *J*-integral rests in its path-independence, demonstrated by Rice, which allows a direct evaluation by choosing properly the integration path Γ. Exploiting this fundamental property, an energy-rate interpretation of *J*-integral is possible when the yielded zone near the crack tip is small, if compared with the representative dimensions of the problem. In fact, both in the case of linear elasticity and also in the case of small-scale yielding, the following relation holds:

$$J = G = \frac{K^2}{E} \tag{1.11}$$

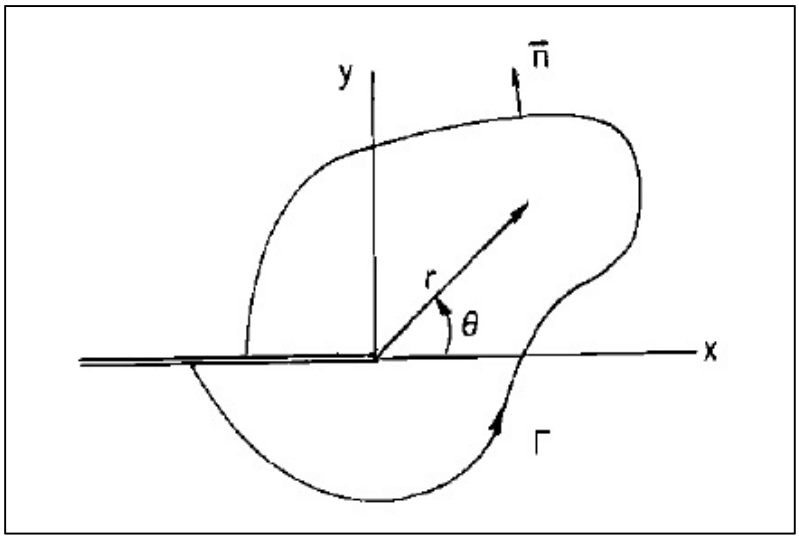

Figure 1.4 – Arbitrary line integral contour [21]

Hutchinson, Rice and Rosengren independently proved that the *J*-integral characterizes the crack tip stress-strain field (called HRR field) in nonlinear materials as follows:

$$\sigma_{ij} = \left(\frac{{\sigma_0}^n J}{\alpha\varepsilon_0 I_n r}\right)^{\frac{1}{n+1}} \widetilde{\sigma_{ij}}(\theta) \qquad (1.12.\text{a})$$

$$\varepsilon_{ij} = \frac{\alpha\varepsilon_0}{{\sigma_0}^n}\left(\frac{{\sigma_0}^n J}{\alpha\varepsilon_0 I_n r}\right)^{\frac{n}{n+1}} \widetilde{\varepsilon_{ij}}(\theta) \qquad (1.12.\text{b})$$

where $\widetilde{\sigma_{ij}}(\theta)$ and $\widetilde{\varepsilon_{ij}}(\theta)$ are angular functions, r is the distance from the crack tip, and I_n is a function of the hardening exponent n of the Ramberg-Osgood constitutive law (1.8), on which depends the strength of the singularity. Because of the more ductile behaviour due to $n > 1$, the relief of crack-tip stress singularity is observed by comparing HRR $-1/(n+1)$ and LEFM exponents $-1/2$.

Assuming n=1, $(\alpha\varepsilon_0/\sigma_0) = 1/E$, and $J = \mathcal{G}$ as suggested by eq. (1.11), we obtain the elastic solution. In this context, elastic situation can be seen as only a particular case of a nonlinear elastic material. Therefore, J can be interpreted as the nonlinear analog to the stress-intensity factor K of LEFM as well as a strain energy release rate.

Focusing on the energy-rate interpretation, it may be shown that J represents the potential energy release rate per unit area of crack advancement in a through-thickness cracked body:

$$J = -\frac{1}{B}\frac{\mathrm{d}U}{\mathrm{d}a} \qquad (1.13)$$

where B is the thickness of the body, U is the potential energy and a is the crack length. Rice pointed out that the interpretation of the J-integral as energy release rate available to crack growth can be extended to plasticity as long seen as nonlinear elasticity, i.e. restricting to monotonically increasing loads without plastic unloadings. With plasticity included, J still remains a crack tip parameter, but it loses its physical meaning as energy potentially available to grow the crack. As an energy comparison, J may still be interpreted as potential energy difference between two identically loaded bodies with incrementally different crack lengths, a and $a + \mathrm{d}a$.

As just done for nonlinear materials with a constitutive relationship in the Ramberg-Osgood form of Eq. (1.8), we will try to extend the fracture mechanics concepts to situations where significant creep deformations occur. Particularly, a new crack-tip parameter will be discussed, considering the analogies between elastic-plastic fracture mechanics (E.P.F.M.) and the so-called time-dependent fracture mechanics (T.D.F.M.).

Based on the analysis of the behaviour of a material undergoing creep deformation, mainly done in the second section of this chapter, the creep constitutive law of Eq. (1.1) is assumed everywhere in a cracked body as well:

$$\dot{\varepsilon} = A\sigma^n \tag{1.14}$$

where $\dot{\varepsilon}$ is the secondary creep strain rate, σ is the applied stress, n is the stress sensitivity and A is a coefficient.

Starting from this assumption, it can be observed that eq. (1.14) is in close agreement with eq. (1.8) relating the crack-tip stress and strains. More precisely,

neglecting the elastic contribution in eq. (1.8), replacing the term $\alpha\varepsilon_0/{\sigma_0}^n$ by the constant A and the strain ε by the strain rate $\dot{\varepsilon}$, eq. (1.14) is obtained. In the case of creeping materials, the exponent n gives an indication of the stress sensitivity of creep, while in the other case it is defined as the strain hardening exponent. Therefore, analogous power-law constitutive relationships can be recognized for plasticity and creep.

Based on this considerable analogy, independently, Landes and Begley [21] and Nikbin, Webster, Turner ([25], [26]) defined a creep-equivalent to the *J*-integral in the following manner:

$$C^* = \dot{J} = \int_{\Gamma} W^* \,\mathrm{dy} - T_\mathrm{i}\left(\frac{\partial \dot{u}_\mathrm{i}}{\partial \mathrm{y}}\right)\mathrm{ds} \tag{1.15}$$

where

$$W^* = \int_0^{\dot{\varepsilon}_\mathrm{ij}} \sigma_\mathrm{ij}\ \mathrm{d}\,\dot{\varepsilon}_\mathrm{ij} \tag{1.16}$$

W^* is the strain energy rate density associated with the point stress σ_ij and strain rate $\dot{\varepsilon}_\mathrm{ij}$, while T_i and Γ are still the traction vector and path already defined for *J*-integral.

This energy rate line integral defined with eq. (1.15) has been called C^* by the first authors, and $\dot{J}$ by the others because of its physical dimension. In this work, the C^* notation is preferred, to prevent confusion with *dJ/dt*. In any case, it represents the creep equivalent of the energy line *J*-integral. In fact, looking at eq. (1.15), C^* is obtained from *J* by replacing the strain and displacement quantities with their time rates, and stress remains as stress. It can be shown that also C^*

integral is path independent, and can be computed along arbitrary contours surrounding the crack tip.

Exploiting the mathematical analogy between *J*-integral and *C**-integral, two fundamental consequences drawn in literature will be discussed here below.

(A) Relationship between *C-integral and the crack-tip stress field**

By analogy with the HRR stress field, previously defined for elastic-plastic fracture mechanics, it is found that the *C**-integral is able to uniquely characterize the magnitude of the stress and strain rate fields at the crack tip:

$$\sigma_{ij} = \left(\frac{C^*}{AI_n r}\right)^{\frac{1}{n+1}} \widetilde{\sigma_{ij}}(\theta) \qquad (1.17.a)$$

$$\varepsilon_{ij} = A\left(\frac{C^*}{AI_n r}\right)^{\frac{n}{n+1}} \widetilde{\varepsilon_{ij}}(\theta) \qquad (1.17.b)$$

Again, the stress singularity at the crack tip is different from -1/2 (elastic), and in this case it depends on the creep stress sensitivity of the material.

(B) Energy rate interpretation of *C-integral**

An energetic definition of *C**-integral is given as follows:

$$C^* = -\frac{1}{B}\frac{dU^*}{da} \qquad (1.18)$$

where B is the thickness of the body, U^* is the potential energy rate and a is the crack length. Basically, it can be defined as the rate of decrease of potential energy rate with respect to crack length.

On the basis of this overview regarding several fracture mechanics parameters, it seems reasonable adopting the C^*-integral as controlling parameter for creep crack growth rate. Landes and Begley [21], published results obtained testing a discalloy at 650°C, attempting a correlation between CCGR and the energy rate line integral. Two different specimen geometries were tested, a centre cracked panel (CCP) and a wedge opening loading specimen (1T-CT). The authors made a comparison with other correlating parameter previously used, namely stress intensity factor and net section stress.

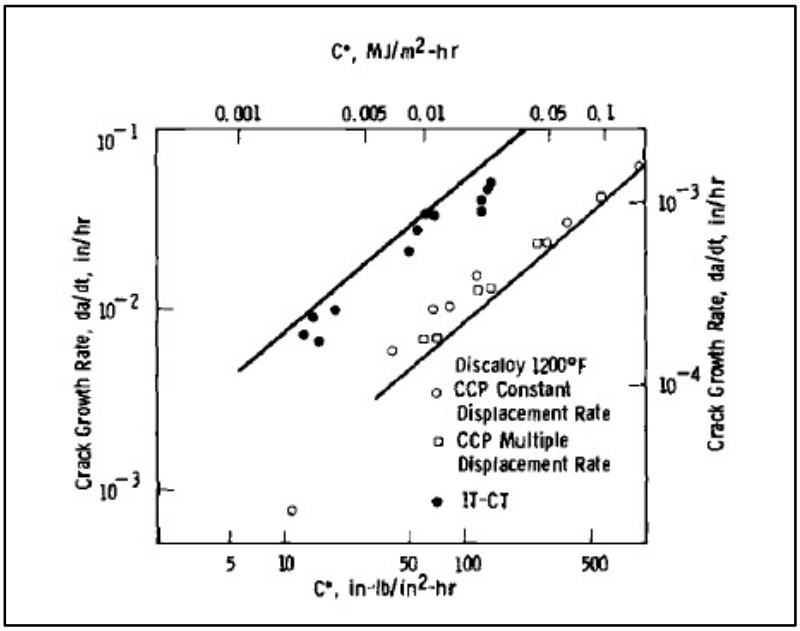

Figure 1.5 – da/dt–C^* correlation [21]

Figure 1.5 shows the results obtained by using the C^*-integral as controlling parameter, considering both specimens type used. Data points are well correlated by a straight line, when CCGR is plotted against C^* parameter, in a log-log diagram. Therefore, the correlation was provided by the following equation:

$$\frac{\mathrm{d}a}{\mathrm{d}t} = D_0 C^{*\phi} \tag{1.19}$$

where $\mathrm{d}a/\mathrm{d}t$ is the CCGR, C^* is the controlling parameter, D_0 and ϕ are coefficients, with ϕ more or less equal to 1.

It can be seen that figure 1.5 provides a scatter in growth rate about a factor of 5, for a given value of C^*. Conversely, when CCGR was plotted agains stress intensity factor, or net section stress, the scatterband was larger, about a factor of 30. Furthermore, in the latter case, the range of the controlling parameter providing a given value of growth, was completely different between the two specimen geometry tested. Therefore, the correlation can be retained successful, especially if compared with that obtained by using stress intensity factor, or net section stress. Nevertheless, looking at fig 1.5 a certain deviation from the straight line was observed for the slowest tests, i.e. a tail part of the curve. For this reason, the authors raised an important question about the existence of a threshold value of C^*, below which cracks don't propagate under creep conditions. The threshold parameter would be in agreement with the threshold value of ΔK, defined for fatigue.

Later, Harper and Ellison [17] found a similar correlation between creep crack growth rate and the C^*-integral. The authors conducted an experimental programme on a 1Cr Mo V steel, tested in air at 565 °C. Tests were carried out on

SEN (single edge notch) and CT (compact tension) specimens. Experimental results are shown in fig. 1.7 and 1.8 for SEN and CT specimens, respectively.

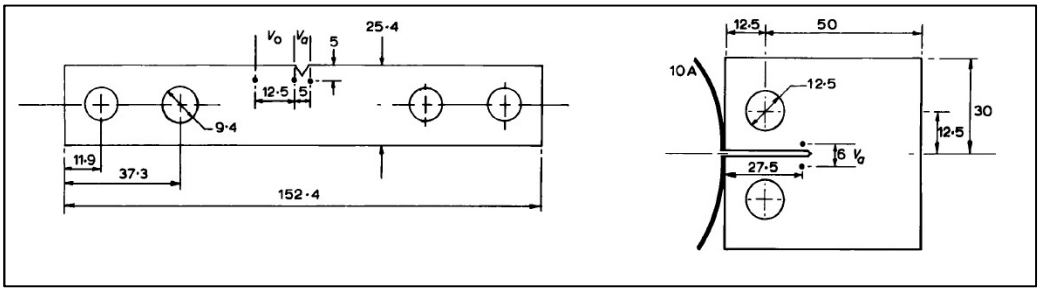

Figure 1.6 – Test specimens geometry [17]

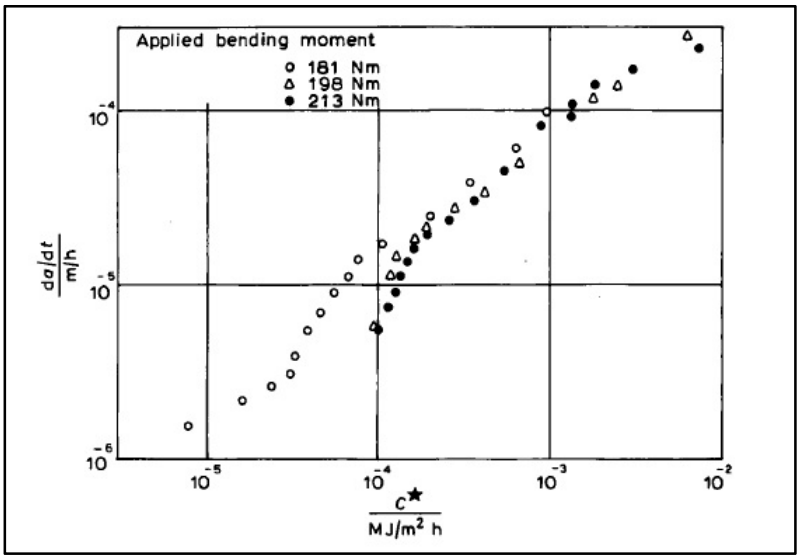

Figure 1.7 - d*a*/d*t*–*C** correlation for SEN specimen [17]

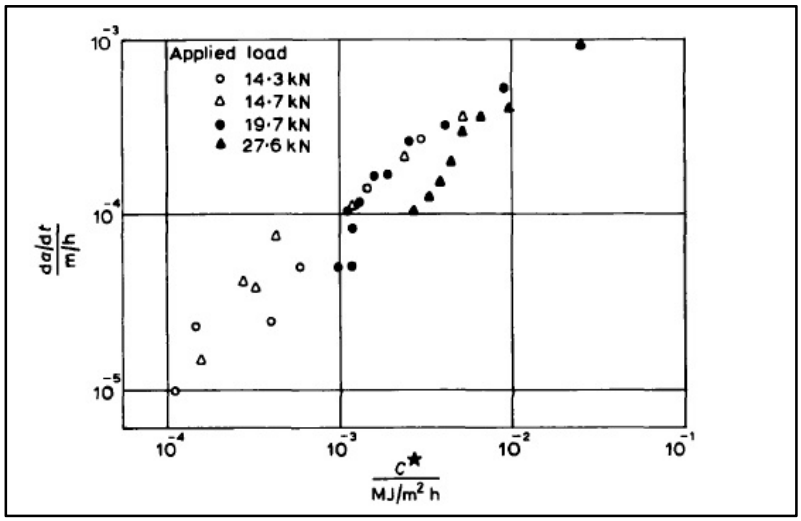

Figure 1.8 - d*a*/d*t*–*C** correlation for CT specimen [17]

As it can be seen, the overall agreement is very good. Once more, in according to the results of Landes and Begley, deviations at low crack growth rates can be observed, providing a change in slope. About this, the authors noticed a certain relationship between the change in slope in the d*a*/d*t* vs *C** diagram and the change in slope in the displacement rate vs time diagram. However, a clear explanation of the nosing behaviour was not provided.

In this context, we should also mention the pioneering work done by Saxena. In Saxena [29], the *C**-integral method has been used to characterize creep crack growth rate of 304 stainless steel, at 594 °C. Centre crack tension (CCT) and compact type (CT) specimens were used. The d*a*/d*t* vs *C** correlation is plotted in fig. 1.9, showing an approximate linear relationship, in according to eq. (1.19).

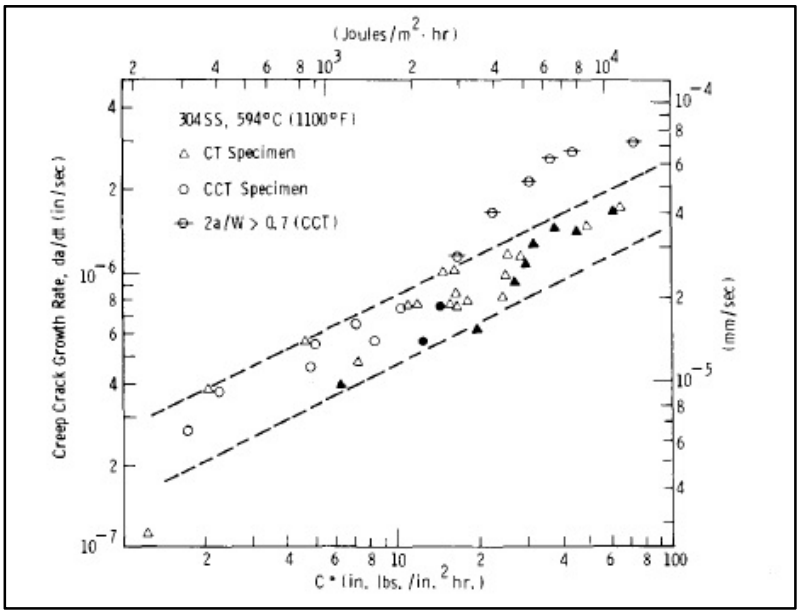

Figure 1.9 - d*a*/d*t*–*C** correlation [29]

All the data lie within a narrow scatterband, in fact the scatter in growth rates was about a factor of 1.4. So, the influence of the specimen geometry was not remarkable. The author states *C**-integral as a promising candidate parameter for characterizing creep crack growth rate.

In Saxena [31] a contrasting result was obtained by the author, carrying out creep crack growth tests on SEN specimens of 316 stainless steel, at temperature of 594 °C. Experimental results showed no correlation of CCGR with the *C**-integral, but with the *J*-integral. This latter parameter was calculated taking into account both the elastic and plastic contribution. In that case, a correlation between d*a*/d*t* and *J* was noticed, very similar to that characterizing stress corrosion cracking.

Nonetheless, the latter could be considered as an isolate one. In the following years, the same author made a lot of efforts to understand creep behaviour for a

wide range of creep conditions, from small scale creep (SSC) to extensive steady-state creep (EC). Following this purpose, Saxena [30] proposed a new crack tip parameter, namely the C_t parameter, for characterizing CCGR. Although some interesting results and observations, the use of the classical C^*-integral has been confirmed.

At this point, after this overview about several fracture mechanics parameter proposed, some conclusions can be drawn. As previously discussed, either the stress intensity factor, or the net section stress, is able to characterize uniquely creep crack growth rate. Generally, it is observed that for relatively "creep brittle" materials, the stress intensity factor K provides a better correlation. On the other hand, when large creep deformation occurs, namely for materials very sensitive to creep, net section stress σ_N seems to be the best correlating parameter. Then, we can conclude that the controlling parameter should be defined in according to the creep sensitivity (ductility) of the tested material. This is not surprising as creep sensitivity affects the amount of redistribution of the initial elastic stresses at the crack tip.

In the "brittle case", when stress redistribution is not so pronounced, the stress intensity factor is still able to describe the stress concentration at the crack tip embedded in an elastic body. For this reason, it correlates well with CCGR. In the other extreme, in the "ductile case", stress redistribution is so relevant that the stress intensity factor is not appropriate in describing the stress field at the crack tip. For sufficient creep ductility, and high value of n, stresses at the crack tip will approach the net section stress (or reference stress), implying a net section rupture rather than a crack propagation problem. In this case, CCGR seems to be well correlated by the net section stress.

Nevertheless, these can be considered only as two extreme conditions. It is necessary a new approach, able to encompass all the "creep ductility conditions", taking into account the pronounced time-dependent nature of the phenomenon. When creep deformation becomes large, neither *K* or *J* is able to take into account time-dependent creep deformation, because it is not included in their formulation. The previous crack-tip parameters lose its significance, pointing out the inapplicability of Linear Elastic Fracture Mechanics (L.E.F.M.) and Elastic Plastic Fracture mechanics (E.P.F.M.) to predict crack growth rate.

Following this purpose, a new crack tip parameter has been introduced, which is the energy rate line *C**-integral. With this parameter, a new branch of fracture mechanics, i.e. Time Dependent Fracture Mechanics (T.D.F.M.), has been identified. In this section, the main concepts of this new branch (stress-fiend and energy interpretation) have been discussed, considering the strong mathematical analogy between T.D.F.M. and E.P.F.M.

Considering the theoretical framework supporting this parameter, several authors attempted to use it as controlling parameter for creep crack growth rate. The correlation has been successful, as it can be seen.

Particularly, an attraction of the *C**-integral method is that it seems consistent with the *K* approach for "creep brittle" circumstances and with the net section stress approach when creep strain governs the problem. As observed by Smith and Webster [35], it seems able to characterize crack growth rate encompassing all the creep ductility conditions.

1.4 Creep as a thermally activated process: Derivation of the Q* parameter

Also in Japan, during the end of the last century, several studies have been made in order to provide a characterization of creep crack growth rate at high temperatures. At the beginning, several attempts have been made using a fracture mechanics approach, as described in the previous section of this work. One of the first work about this issue has been done by Koterazawa and Iwata [19]. They conducted a fracture mechanics study on creep crack propagation of a 304 stainless steel under constant tensile stress at a temperature of 650 °C. In detail, two specimen geometries (circumferentially notched round bar and double edge notched plate) were tested in air, to define the fracture mechanics parameter controlling CCGR. Crack propagation rates (calculated graphically from crack length versus net time curves) were plotted as a function of net section stress σ_N and stress intensity factor K. Experimental results showed that a better correlation was achieved adopting the stress intensity factor K as controlling parameter.

Immediately after, Koterazawa and Mori [20] published another work about this issue. In this article, the authors dealt a more complete discussion about the applicability of several fracture mechanics parameters characterizing creep crack growth, including the modified J-integral (or C^*-integral) previously introduced. Base Material tested was still the same, 304 stainless steel, but in this case three different heats were provided giving different mechanical properties. With respect to the preceding work, a wider range of specimen geometries was used (three types of double edge notched specimens of different size, a type of centre notched specimen, two types of single edge notched specimens). Tests were conducted in

air at the temperature of 650 °C. Again, crack growth rates were plotted against its controlling parameter, respectively net section stress σ_N, stress intensity factor K and C^*-integral. It is shown that C^*-integral gave the best correlation including in a narrow band all the data points related to each specimen geometry. Also in this case, as discussed in the previous section for C^*-integral, when this parameter has been correlated with crack growth rate, the experimental curve revealed a nose part. In subsequent years, a more extensive investigation has been carried out considering additional experimental data. Yokobori T. and Sakata ([40], [41], [42]) conducted an experimental work regarding the behaviour of 304 stainless steel (double edge notched specimen) under creep, fatigue and creep-fatigue interaction conditions at high temperature, in vacuum.

Crack growth rate on a time basis was plotted against stress intensity factor as controlling parameter. It was pointed out that the relation between logarithm of crack growth rate and logarithm of stress intensity factor may be divided in three regions, both for creep and fatigue. Then the authors noticed that these curves deviate in some systematic trend by varying gross stress, holding time and temperature.

Focusing our attention on creep results, we will discuss only the effect of gross stress and temperature. In detail, considering the region II of the curve, it was shown that creep crack growth rate increases with increase of gross section stress and temperature (fig. 1.10). Plotting creep crack growth rate against net section stress, the authors noticed the same deviations. So, the conclusion of this experimental work was that creep crack growth rate could not be described uniquely in terms of stress intensity factor K or net section stress σ_N with respect

to fracture mechanics parameter. It was necessary to find a unifying approach, in order to include dependencies of creep crack growth rate on gross section stress σ_g and absolute temperature T.

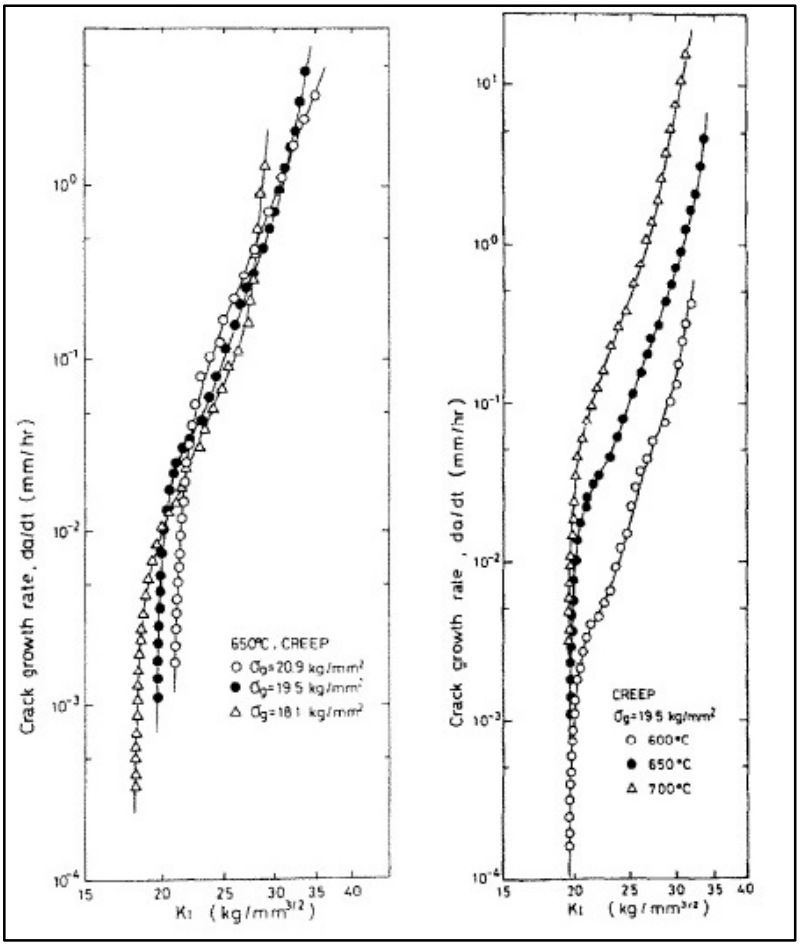

Figure 1.9 – Tests results reported in [40]

Assuming this as starting point, a more detailed analysis can be found in [42]. Based on a series of previous experimental data, the authors attempt to relate creep crack growth rate da/dt to the stress intensity factor (calculated considering

an effective crack length a_{eff}), applied gross stress and temperature. They firstly explored the relation between crack growth rate and fracture mechanics parameter at specified temperature. For the material subject of study, 304 stainless steel, it was found:

$$\frac{\mathrm{d}a}{\mathrm{d}t} = 8.55 \times 10^{-22} \sigma_g{}^{5.64} \left(\alpha \sqrt{a_{eff}}\, \sigma_g\right)^{9.20} \tag{1.20}$$

The temperature dependence of creep crack growth rate is studied plotting the logarithm of da/dt vs the logarithm of $\alpha\sqrt{a_{eff}}\sigma_g$ with temperature as independent parameter at a specified value of gross section stress. An "Arrhenius type" equation hold:

$$\frac{\mathrm{d}a}{\mathrm{d}t} = A^* \exp\left(-\frac{\Delta H_\mathrm{g}}{\mathrm{R}T}\right) \tag{1.21}$$

A^* is a constant dependent on σ_g, R is the gas constant, T is the absolute temperature and ΔHg is the apparent activation energy for crack extension. The last is expressed as follow:

$$\Delta H_\mathrm{g} = \Delta f_1 - \Delta f_2 \ln\left(\frac{\alpha\sqrt{a_{eff}}\, \sigma_g}{G\sqrt{\mathrm{b}}}\right) \tag{1.22}$$

where G is the modulus of rigidity, b the Burgers vector, Δf_1 and Δf_2 are material constants.

To conclude, considering equations (1.20), (1.21) and (1.22), creep crack growth rate for a 304 stainless steel was characterized by the following expression:

$$\frac{\mathrm{d}a}{\mathrm{d}t} = 0.00299\ {\sigma_g}^{5.64} \exp\left(-\frac{7.82 \times 10^4 - 1.68 \times 10^4 \ln\left(\frac{\alpha\sqrt{a_{eff}}\ \sigma_g}{G\sqrt{\mathrm{b}}}\right)}{\mathrm{R}T} \right) \quad (1.23)$$

or by taking logarithm of both sides:

$$\log\frac{\mathrm{d}a}{\mathrm{d}t} = 3.48 + \frac{8.48 \times 10^3}{T}\log\left(\frac{\alpha\sqrt{a_{eff}}\ \sigma_g}{4.66 \times 10^2}\right) + 5.64 \log\ \sigma_g \quad (1.24)$$

Assuming now:

$$P = \frac{8.48 \times 10^3}{T}\log\left(\frac{\alpha\sqrt{a_{eff}}\ \sigma_g}{4.66 \times 10^2}\right) + 5.64 \log\ \sigma_g \quad (1.25)$$

as characterizing parameter, it is established a linear relationship between the logarithm of CCGR and *P*. It is shown that the parameter here proposed correlates fairly well with experimental data. In that work, a correlation similar of eq. (1.23) was obtained also for the mechanisms of fatigue and creep-fatigue interaction.

In the subsequent years, a further assessment was done by A.T. Yokobori and co-workers [39] about CCGR representation. In the work in question, the authors

derived a similar parametric representation of creep crack growth rate, by using the same data reduction scheme. Differently from the previous study, in this case stress intensity factor is evaluated considering an equivalent crack length equal to the sum of the pre-notch length and the actual crack length. By proceeding in this way, CCGR was predicted by the following equation:

$$\frac{\mathrm{d}a}{\mathrm{d}t} = 1.81 \times 10^{-4} {\sigma_g}^{4.14} \exp\left(- \frac{3.59 \times 10^5 - 7.25 \times 10^4 \ln\left(\frac{\alpha\sqrt{a}\,\sigma_g}{G\sqrt{\mathrm{b}}}\right)}{\mathrm{R}T} \right) \quad (1.26)$$

Then, as done for the *P* parameter, *Q* parameter was defined as:

$$Q = \frac{8.74 \times 10^3}{T} \log\left(\frac{K}{1.94 \times 10^2}\right) + 4.14 \log\, \sigma_g \quad (1.27)$$

In contrast to the *P* parameter (1.25), in *Q* parameter (1.27) the stress intensity factor *K* appears as classically defined. As observed for the *P* parameter, the *Q* parameter is able to fit the experimental data very accurately (fig. 1.10).

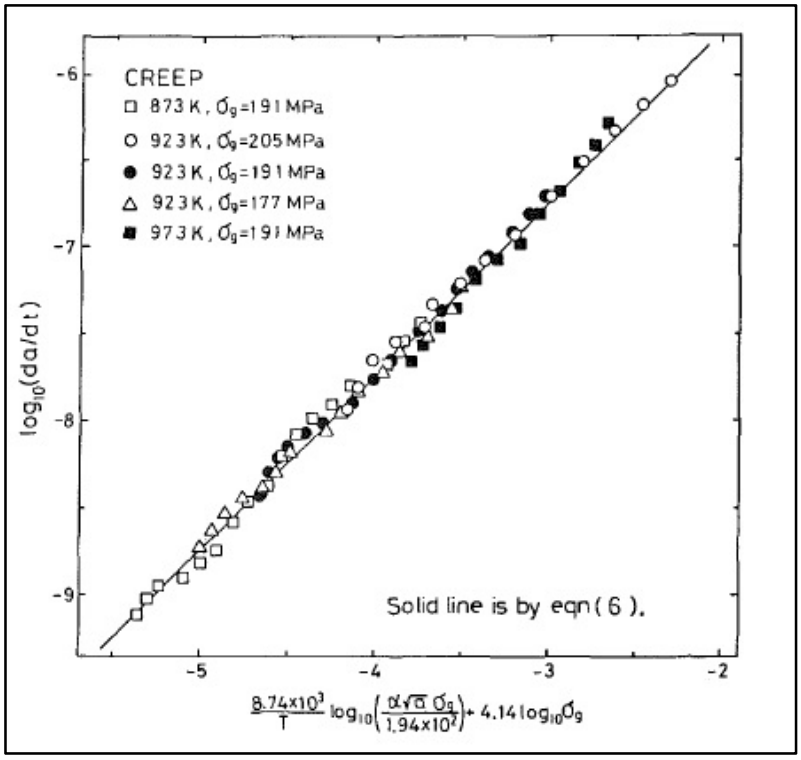

Figure 1.10 – d*a*/d*t* – Q correlation reported in [39]

Until that moment, any consideration about specimen size was done, so size effect was still not included. Further investigations, lead on the revision of the *Q* parameter, such way to include specimen width effect. Particularly, in [38] the authors pointed out the dependence of creep crack growh rate on the specimen size. For a 304 stainless steel, the following relation is proved to be held:

$$\frac{\mathrm{d}a}{\mathrm{d}t} = 652\left(\frac{W}{W_0}\right)^{-2.58} {\sigma_g}^{4.14} \exp\left(-\frac{3.59\times10^5 - 7.25\times10^4 \ln\left(\frac{\alpha\sqrt{a}\,\sigma_g}{G\sqrt{\mathrm{b}}}\right)}{\mathrm{R}T}\right) \qquad (1.28)$$

Now, writing eq. (1.29) as:

$$\frac{\mathrm{d}a}{\mathrm{d}t} = 652 \times 10^{\mathrm{Q}^*} \qquad (1.29)$$

and making a comparison between eq. (1.28) and eq. (1.29), the Q^* parameter for a 304 stainless steel is defined as follow:

$$Q^* = \frac{8.74 \times 10^3}{T} \log\left(\frac{K}{1.94 \times 10^2}\right) + 4.14 \log\ \sigma_g - 2.58 \log\left(\frac{W}{W_0}\right) \qquad (1.30)$$

By taking logarithm of both sides of eq. (1.29) again a linear relationship between the logarithm of CCGR and the controlling parameter is obtained (fig. 1.11). But in this case, the Q^* parameter includes specimen size effect, so it is more suitable for predicting creep crack growth rate.

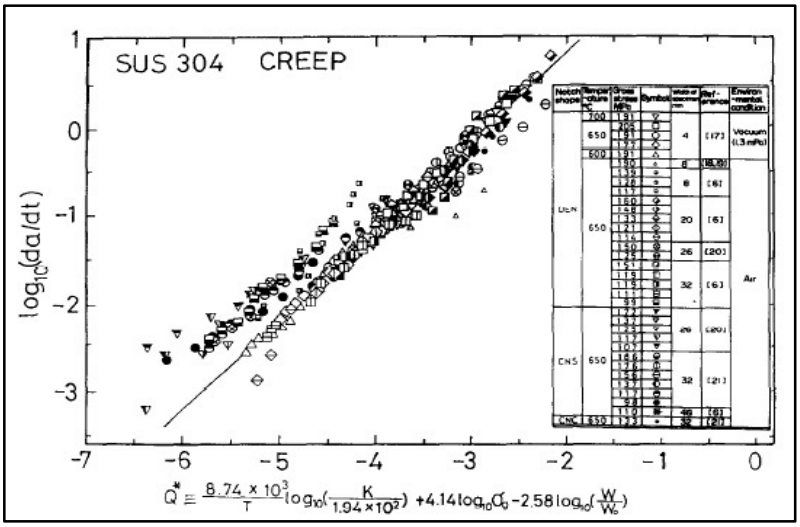

Figure 1.11 - d*a*/d*t* – Q* correlation reported in [38]

The approach just described can be seen as an innovative one. In fact, eq. (1.28) can be written in a more general form as follow:

$$\frac{\mathrm{d}a}{\mathrm{d}t} = B \left(\frac{W}{W_0}\right)^{-\mathrm{l}} {\sigma_g}^{\mathrm{m}} \exp\left[-\frac{\left[\Delta H_f - \mathrm{M} \ln\left(\frac{K}{G\sqrt{\mathrm{b}}}\right)\right]}{\mathrm{R}T}\right] \tag{1.31}$$

or, in the same way:

$$\frac{\mathrm{d}a}{\mathrm{d}t} = B \left(\frac{W}{W_0}\right)^{-\mathrm{l}} {\sigma_g}^{\mathrm{m}} \left(\frac{K}{G\sqrt{\mathrm{b}}}\right)^{\frac{\mathrm{M}}{\mathrm{R}T}} \exp\left(-\frac{\Delta H_f}{\mathrm{R}T}\right) \tag{1.32}$$

where K is the elastic stress intensity factor, σ_g is the applied gross stress, T the absolute temperature, W the specimen width, W_0 the reference specimen width, R is the gas constant, G is the modulus of rigidity, b the Burgers vector while B, l, m, $\mathrm{M} = \alpha_1 - \alpha_2 \mathrm{T}$, and ΔH_f can be considered material constants. Particularly, in eq. (1.32) it is clearly underlined the power-law dependence of the creep crack growth rate on the applied gross stress and stress intensity factor.

It must be noticed that (1.32) can be also written as:

$$\frac{\mathrm{d}a}{\mathrm{d}t} = C_0 K^m \tag{1.33}$$

where C_0 is a constant dependent of σ_g, specimen width W, absolute temperature T and n is the inclination of the straight line obtained plotting logarithm of both sides. It's remarkable that Eq. (1.33) resembles the Paris' law equation.

Rewriting eq. (1.32) in a simpler form:

$$\frac{\mathrm{da}}{\mathrm{dt}} = \mathrm{B}\exp(\mathrm{Q}^*) \tag{1.34}$$

a typical thermally activated equation is found, in which the Q^* parameter is the index of the exponential in the equation of the thermally activated process. In this way, the theoretical meaning of this approach proposed by A.T. Yokobori and colleagues ([37], [38]) is explained. It comes from the assumption that creep crack growth is a thermally activated process.

Then, the final proposed parameter is defined as:

$$Q^* = -\frac{\Delta H_f - \mathrm{M}\ln\left(\frac{K}{G\sqrt{\mathrm{b}}}\right)}{\mathrm{R}T} + \mathrm{m}\log\sigma_g + \mathrm{l}\log\frac{W}{W_0} \tag{1.35}$$

or:

$$Q^* = \frac{\mathrm{M}\log\frac{K}{K_r}}{\mathrm{R}T} + \mathrm{m}\log\sigma_g + \mathrm{l}\log\frac{W}{W_0} \tag{1.36}$$

where:

$$K_r = G\sqrt{\mathrm{b}}\exp\left(\frac{\Delta H_f}{\mathrm{M}}\right) \tag{1.37}$$

As it can be seen, the controlling parameter Q^* is defined in terms of independent variables including stress intensity factor K, applied gross stress σ_g, absolute temperature T and the specimen width W.

To conclude, this newly proposed parameter seems to provide a better correlation with crack growth rate, with respect to other fracture mechanics parameter discussed in the former section (net section stress σ_N, stress intensity factor K, C^*-integral). More precisely, results derived by this empirically-derived correlation, show that crack growth rate is correlated by a simple monotonically increasing linear function of Q^*. The authors showed that all the collected data collapse into a single curve, within a very narrow band. By making a comparison with the C^* representation on a bi-logarithmic scale, no tail part of the curve is revealed at early stage of crack growth, although a threshold value of Q^* could be determined. So, for this reason, Q^* parameter seems to more efficient for predicting creep crack growth rate at high temperatures.

2. SCALING LAWS IN CREEP

2.1 Introduction

As shown in a variety of studies, the structural behaviour and rupture properties of full-scale elements under different loading conditions are mainly extrapolated from laboratory tests carried out on small-scale specimens. In this perspective, creep rupture properties will be studied focusing on the so-called size and scale effects. More precisely, we will deal with the specimen-size dependence of the rupture time for smooth specimens. Afterwards, the crack-size effect on the da/dt vs. C^* relationship will be discussed for notched specimens.

Several physical phenomena, referring to very different application fields, are affected by scaling effects. For instance, anything like that occurs in Fluid Mechanics, where the transition from laminar to turbulent flow is ruled by a dimensionless parameter, the Reynolds number, which predicts scale effects in geometrically similar but different-sized flow situations. Essentially, for given velocity, viscosity and geometry, the same fluid undergoes laminar-to-turbulent transition, by exceeding a certain characteristic linear dimension of the flow, e.g., the pipe diameter in case of pipe flows.

In Solid Mechanics, analogous transition occurs when the structural size is increased. In this case, the transition from plastic flow (ductile) collapse to fracture collapse (separation) is governed by the brittleness number s, introduced by Carpinteri [3] in the framework of Dimensional Analysis. More precisely, a

progressive embrittlement of the structural collapse occurs by increasing the structural size, even if fracture insensitive, or ductile, materials are considered.

Still in the context of scale effects on structural collapse, noticeable advances were made at the end of the last century. On the basis of several experimental evidences, Carpinteri ([5]-[9]) proposed the use of a fractal geometry approach to Fracture Mechanics, where the resisting cross section and the fracture surface at final rupture are modelled as fractal sets with anomalous (non-integer) physical dimensions, instead of considering them as Euclidean surfaces. Following the so-called renormalization procedure, the author introduced new mechanical properties with non-integer dimensions, the renormalized fracture energy $\mathcal{G}_F^*$ and the renormalized tensile strength σ_u^*, that are invariant with respect to a characteristic length scale of the fracture phenomenon, i.e. the specimen size or the crack size. The fractal dimensions of such scale-invariant material constants come from the scaling (power-law) behaviour of the corresponding nominal quantities $\mathcal{G}_F$ and σ_u.

Subsequently, all these concepts have been applied to fatigue. Experimental observations have shown that fatigue phenomenon is affected by scaling effects, both for uncracked (nominally flaw-free) specimens and cracked specimens. These effects have been tackled by means of a dimensional analysis approach by Carpinteri et al. ([10], [11], [14]), providing a generalization of fatigue laws, both for smooth specimens (Wöhler law), and for cracked specimens (Paris law). A more detailed analysis of these effects has been carried out using fractal geometry tools, as previously discussed ([12], [13], [27]). In the latter case, fractal geometry provided a better interpretation of the anomalous behaviour of fatigue-crack growth rates of short cracks.

In the following sections, we will deal with size effects in the creep behaviour of smooth and notched specimens. Firstly, size effects of smooth, i.e. nominally flaw-free, specimens will be analysed. Afterwards, crack size effects on creep crack growth will be discussed. In both cases, we will work on the basis of appropriate experimental evidences, although direct studies in this context are very few. As done for fatigue, a consistent theoretical framework will be proposed, by means of Buckingham's theorem and fractal geometry. Although their underlying theoretical framework is very different, these two approaches will be able to highlight scale effects in the creep phenomenon.

Therefore, the aim of this work is to shed light on several aspects about scaling effects noticeable for creep behaviour, for which a clear theoretical framework is still lacking. Currently, we are not aware about any systematic studies on size effects pro creep phenomenon, so it seems worthwhile to continue research work in this field.

This work will be concluded suggesting several considerations about the influence of material nonlinearity and microstructural disorder on the stress field at the crack tip, and the consequent collapse mechanism. It will be shown that increasing the non-linearity of the material, a transition from brittle-to-ductile failure similar to that obtained by reducing the structural size could be noticed.

2.2 Interpretation of specimen-size effects on σ-t_R curves according to dimensional analysis

As we said before, an interpretation of size effects on creep rupture will be provided on the basis of previous experimental campaigns. Following this purpose,

experimental results published by Goldhoff [16] will be considered. The aim of that work was to discuss both stress concentration and size effects, on creep rupture. Cylindrical specimens of Cr-Mo-V steel were tested in uniaxial tension at very high temperatures, ranging from 482 °C to 593 °C, i.e. under creep conditions. Although the base material was the same, several test specimens with small variations in chemical composition, different heat treatment and mechanical properties have been used. More detailed information are given by the author in his work.

About size effects for smooth specimens, the author tested steel no.2 and steel no.3, as reported in his paper. Steel no.2 was tested at temperature of 482 °C, 538 °C and 593 °C, while steel no. 3 at 538 °C and 593 °C. For each steel, a wide range of specimen size has been investigated, providing a consistent evaluation of size effects. More precisely, round bar specimens of 0.160, 0.253, 0.505 and 1.128 in. have been used for smooth testing, exploring a specimen size variation of about one order of magnitude.

Experimental results are shown in Fig. 2.1, where the σ-t_R curve is represented as a function of temperature and bar size, for both steel no.2 and steel no. 3. Small, but systematic variation of these curves can be observed, by varying the characteristic specimen size, i.e. the specimen diameter.

Looking in detail at fig. 2.1, for steel no.2 a reduction of the creep strength is noticed when the specimen size increases. Considering results for steel no.2 at 538 °C, the author reported a linear dependence between rupture strength at 1000 h and the reciprocal of bar diameter. This result is in accordance with the pioneering work mostly done at the end of this century, mentioned in the previous section 2.1.

It also to be noted the behaviour of steel no. 3 at 538 °C, with an increase of creep strength by increasing specimen size, apparently inconsistent with numerous experimental findings of size effects on nominal tensile strength. However, this result cannot be ignored, making further experimental studies on creep size effects much-needed to validate the theoretical framework presented here.

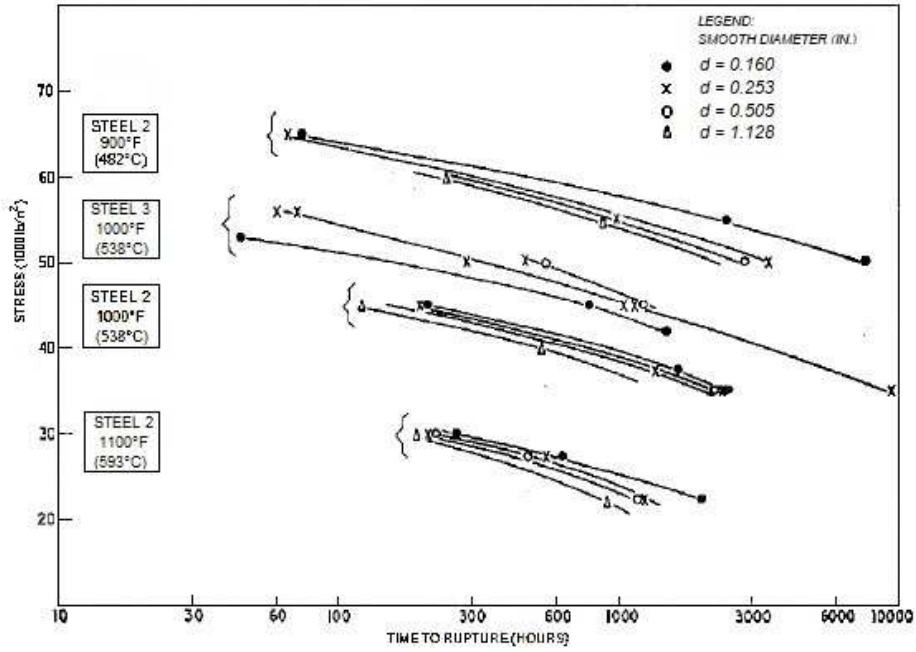

Figure 2.1 – Creep rupture results for smooth specimens [16]

Based on these evidences, in this section we will try to tackle these effects, by means of dimensional approach already used for fatigue rupture. In this sense, the first step is to identify a functional dependence between the output parameter characterizing the phenomenon, and input parameters able to describe completely the phenomenon under observation. For the case of creep rupture of uncracked

specimens, the output parameter is the rupture time t_R, and the following functional dependence can be stated:

$$t_R = \Psi\ (\sigma, T;\ \sigma_u, \sigma_{th}, K_C, \chi, T_M; b) \qquad (2.1)$$

where the governing variables into round brackets are summarized in Tab. 2.1, with their physical dimensions expressed in the Force-Length-Time-Temperature system.

Variable	Definition	Dimensions
σ	Applied Stress	$[F][L]^{-2}$
T	Temperature	$[\theta]$
σ_u	Ultimate tensile strength	$[F][L]^{-2}$
σ_{th}	Creep threshold	$[F][L]^{-2}$
K_C	Fracture toughness	$[F][L]^{-3/2}$
χ	Thermal diffusivity	$[L]^2[T]^{-1}$
T_M	Melting Temperature	$[\theta]$
b	Specimen size	[L]

Table 2.1 – Input parameters and physical dimensions

Looking at the whole set of dependent variables, we can identify three kind of parameters. Two of them, σ and T, can be considered as "loading" parameters, because they depend on the testing conditions. Others, as $\sigma_u, \sigma_{th}, K_C, \chi$ and T_M can

be considered as “material properties”. Finally we find the characteristic specimen size b, on which we focus our attention.

In order to apply Buckingham’s Π Theorem, it is necessary to define an adequate subset of independent variables, in according to the number of basic dimensions which describe the phenomenon. As for Fluid Dynamics, in the case of creep four basic dimensions are used, usually taken to be Force F, length l, time t and temperature T. The following four independent variables are considered, K_C, σ_u, χ and T_M, along with their respective physical dimension expressed in Tab. 2.1.

For sake of completeness, the independence of these variables is proved as follow. Firstly, it has to be noticed that only the variable T_M contains the basic dimension θ, so T_M is certainly independent on the other three variables. For this reason, the independence of the remaining variables K_C, σ_u, χ is proved by providing that their combination cannot give a dimensionless group. More precisely:

$$[\mathrm{K_C}]^{\alpha}[\sigma_\mathrm{u}]^{\beta}[\chi]^{\gamma} = \left([\mathrm{F}][\mathrm{L}]^{-3/2}\right)^{\alpha}([\mathrm{F}][\mathrm{L}]^{-2})^{\beta}([\mathrm{L}]^{2}[\mathrm{T}]^{-1})^{\gamma} = [\mathrm{F}]^{0}[\mathrm{L}]^{0}[\mathrm{T}]^{0} = [0] \tag{2.2}$$

Equating the exponent of each basic dimension, it is obtained:

Force: $$\alpha + \beta = 0 \tag{2.3.a}$$

Length: $$-\frac{3}{2}\alpha - 2\beta + 2\gamma = 0 \tag{2.3.b}$$

Time: $$-\gamma = 0 \tag{2.3.c}$$

The set of Eq. (2.3.a), (2.3.b), (2.3.c) represents a homogeneous system of three linear equations with three unknows (α, β and γ), which solution is given by

Rouche'-Capelli theorem. Following this route, the only nontrivial solution is obtained only if:

$$\det[\mathrm{A}] = \det\begin{bmatrix} 1 & 1 & 0 \\ -3/2 & -2 & 2 \\ 0 & 0 & -1 \end{bmatrix} \neq 0 \qquad (2.4)$$

By calculating, we obtain det[A] = 1/2, therefore the independence is proved. We can conclude that the choice of K_C, σ_u, χ as independent variables is suitable.

Going back to eq. (2.1) and by applying Buckingham's Π Theorem, a dimensionless relationship can be established between the governing variables:

$$t_R = \frac{1}{\chi}\left(\frac{K_C}{\sigma_u}\right)^4 \Psi_1 \left(\frac{\sigma}{\sigma_u}, \frac{\sigma_{th}}{\sigma_u}, \frac{T}{T_M}, \left(\frac{\sigma_u}{K_C}\right)^2 b\right) \qquad (2.5)$$

Each dimensional variable has been made dimensionless, by using an appropriate combination of power law of the four independent variable, providing also that Eq. (2.5) is dimensionally homogeneous, having both sides the dimension of a time. Making a comparison between eq. (2.1) and eq. (2.5), it can be noticed that by applying Buckingham's Theorem, the involved parameters are reduced by 4, the number of basic dimensions previously discussed.

Looking for a further reduction of the involved parameters in this generalized law, we should deal a discussion about complete or incomplete self-similarity. As noticed by Barenblatt [2], and then applied by Carpinteri et al. ([10], [11], [14]), for fatigue, we speak about complete self-similarity in a generic parameter, when a finite non-zero limit of the function Ψ exists, for very large or very small values of the corresponding parameter. In this case, the parameter is considered as non-

essential, and can be removed from the analysis. Conversely, when the limit of the function Ψ tends to zero or infinity, a power-law relationship can be hold, describing the central regime between two limit asymptotic representation. In this case we talk about incomplete self-similarity.

Following this route, we obtain:

$$t_R = \frac{1}{\chi}\left(\frac{K_C}{\sigma_u}\right)^4 \Psi_2\left(\frac{\sigma_{th}}{\sigma_u}, \frac{T}{T_M}\right)\left(\left(\frac{\sigma_u}{K_C}\right)^2 b\right)^{\alpha_2}\left(\frac{\sigma}{\sigma_u}\right)^{\alpha_1} = B\sigma^{\alpha_1} \qquad (2.6)$$

It has to be noticed that assuming incomplete self-similarity, allow to make explicit the power law dependence of the rupture time t_R on the applied stress σ, in the same form of eq. (1.4). In this sense, it can be said that Buckingham's Theorem lead to a generalized law for creep rupture. The additional information is that the "constant" B depends on the characteristic specimen size b, other than material properties.

With regards to experimental results previously shown for steel no.2, they can be easily tackled, on the condition that the exponent α_2 is negative. More precisely, looking at eq. (2.6), the scaling effect is ruled by the dimensionless group:

$$\left(\frac{\sigma_u}{K_C}\right)^2 b = \frac{1}{s^2} \simeq \frac{b}{a_0} \qquad (2.7)$$

where s is the brittleness number introduced by Carpinteri [3] which rules the transition from plastic collapse through instable crack propagation, and a_0 is the characteristic length defined in according to Griffith energetic approach. Introducing eq. (2.7) in eq. (2.6):

$$t_R = \frac{1}{\chi}\left(\frac{K_C}{\sigma_u}\right)^4 \Psi_2\left(\frac{\sigma_{th}}{\sigma_u}, \frac{T}{T_M}\right)\left(\frac{b}{a_0}\right)^{\alpha_2}\left(\frac{\sigma}{\sigma_u}\right)^{\alpha_1} = B\sigma^{\alpha_1} \qquad (2.8)$$

In terms of scaling effect, this result is basically the same of that obtained for fatigue, since we are dealing creep in the context of L.E.F.M. In fact, it comes from the assumption of the stress intensity factor *K* as a controlling parameter, which is an elastic crack-tip parameter. Things will change when dimensional analysis will be applied in the context of Time Dependent Fracture Mechanics (T.D.F.M.), i.e. assuming the *C**-integral as governing parameter for creep phenomenon.

In fact, applying the same approach in the framework of T.D.F.M., we can write:

$$t_R = \Psi\ (\sigma, T;\ \sigma_u, \sigma_{th}, C_C^*, A, T_M; b) \qquad (2.9)$$

Making a comparison with eq. (2.1), one can see that the critical parameter is now C_C^* instead of *K*, showing that we are operating in the context of Nonlinear Fracture Mechanics. Further, it is to note that the thermal diffusivity χ is replaced by *A*, constitutive parameter for creep, which appears in Norton's law (eq. 1.1). Physical dimension of each parameter in eq. (2.9) can be found in Tab. 2.2.

Variable	Definition	Dimensions
σ	Applied Stress	$[F][L]^{-2}$
T	Temperature	$[\theta]$
σ_u	Ultimate tensile strength	$[F][L]^{-2}$
σ_{th}	Creep threshold	$[F][L]^{-2}$
C_C^*	Critical C* integral	$[F][L]^{-1}[T]^{-1}$
A	Thermal diffusivity	$[F]^{-n}[L]^{2n}[T]^{-1}$
T_M	Melting Temperature	$[\theta]$
b	Specimen size	[L]

Table 2.2 - – Input parameters and physical dimensions

Again, by applying Buckingham's Π Theorem, eq. (2.9) can be transformed in a new dimensionless relationship between all the parameters mentioned, providing also a reduction by 4 of the all parameters involved:

$$t_R = \frac{1}{A{\sigma_u}^n}\,\Psi_1\left(\frac{\sigma}{\sigma_u}, \frac{\sigma_{cl}}{\sigma_u}, \frac{T}{T_M}, \frac{A{\sigma_u}^{n+1}}{C_C^*}b\right) \qquad (2.10)$$

Similarly to the previous case, the parameters σ_u, C_C^*, A and T_M have been used as independent variables. It can be shown that these 4 parameters are independent.

Assuming incomplete self similarity:

$$t_R = \frac{1}{A{\sigma_u}^n}\Psi_2\left(\frac{\sigma_{cl}}{\sigma_u}, \frac{T}{T_M}\right)\left(\frac{A{\sigma_u}^{n+1}}{C_C^*}b\right)^{\alpha_2}\left(\frac{\sigma}{\sigma_u}\right)^{\alpha_1} = B^*\sigma^{\alpha_1} \qquad (2.11)$$

the power law dependence of the phenomenon is stressed again, as in eq. (2.6)

Again, we found a constant B which depends on the specimen size b. In this case, the scaling effect is governed by the following dimensionless group:

$$\frac{A\sigma_u{}^{n+1}}{C_C^*}b \tag{2.12}$$

providing the desired effect, when α_2 is negative.

In other words, we defined a new "characteristic length" which rules the size effects for creep. Although in Eq. (2.12) different terms appear with respect to Eq. (2.7), one can see that these two dimensionless groups are comparable. Considering the well-known Irwin's relationship, Eq. (2.12) can be expressed in the following form:

$$\left(\frac{\sigma_u}{K_C}\right)^2 b = \frac{\sigma_u{}^2}{G_C E}b \tag{2.13}$$

Now, making a comparison between Eq. (2.7) and (2.13), it can be seen that they are conceptually the same. In both cases, the critical value of the controlling energetic parameter appears at the denominator. Further, the same dependence on the ultimate tensile strength is obtained if n=1. Finally, it has to be noticed that the constitutive parameter A plays the same role of $1/E$ in the constitutive laws. Therefore, we can state the suitability of the dimensionless group defined in eq. (2.13), governing creep phenomenon.

Concluding this section, we can say that also for creep dimensional analysis approach enables one to tackle size effects, making predictable the behaviour of a

full-scale system by testing a geometrically similar small-scale model, i.e. laboratory scale specimen. Although these scaling effects on the specimen size are not clear, as confirm by experimental tests previously discussed, the dimensional analysis approach seems to be a suitable tool for their prediction.

2.3 Interpretation of specimen-size effects on σ-t_R curve according to fractal geometry

In this section, we will try to interpret specimen size effects on rupture time, by means of fractal geometry concepts. In other words, the aim remains the same of the previous section, but a different theoretical approach will be used. These concepts have been applied in solid mechanics, providing a better understanding of critical phenomena in this field. More precisely, the approach is based on the definition of new critical mechanical parameters, with non-integer physical dimensions, as a scale invariant property of the material. This procedure, i.e. Renormalization Group Theory, already used for fatigue, will be adjusted for creep. Cause of the lack of experimental data, only monofractal scaling laws will be proposed.

Firstly, the following law describing creep rupture is assumed:

$$t_R = B_0 \left(\frac{\sigma_0}{\sigma}\right)^p \tag{2.14}$$

This relationship is equal to eq. (1.4), but the constant B is assumed equal to ${B_0\sigma_0}^P$, to make explicit the intercept of the σ-t_R curve, conceptually represented in fig. (2.2).

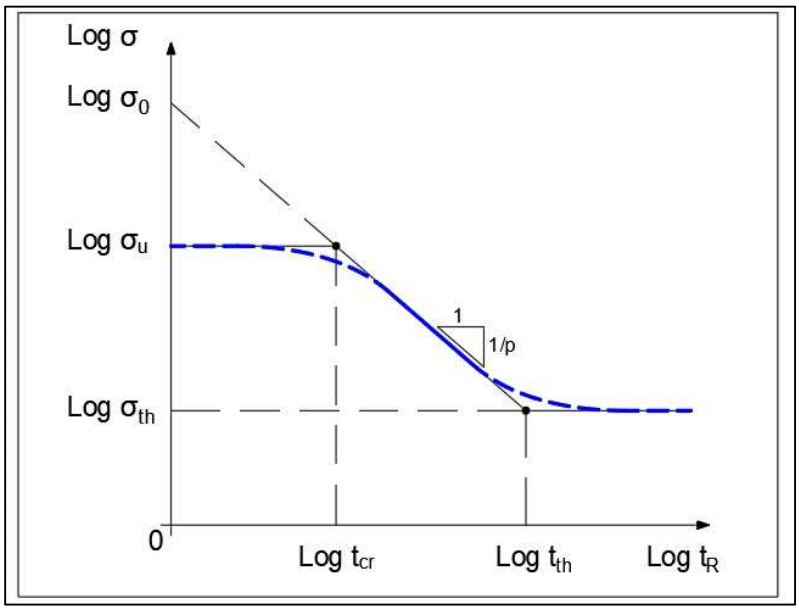

Figure 2.2 - Schematic creep rupture curve

As it can be seen, in Fig. 2.2, two deviations from the central part of the curve, have been introduced. At high stress level, approaching the yielding stress, a first deviation from the power law regime is represented, also in according to observation reported by Garofalo [15]. Further, at low stress level, another deviation occurs, providing longer rupture time t_R, when the applied stress σ becomes lower and lower. In this perspective, we put forward the existence of a threshold stress for creep, below which creep phenomenon doesn't occur. Threshold stress for creep would be the analogous of the fatigue limit $\Delta\sigma_{fl}$ for fatigue, about which the scientific debate is still open. This proposal seems consistent with several experimental results recently carried out.

A straightforward application of the Renormalization Group procedure, permits to derive a scaling law for nominal creep strength. In detail, modelling the

reacting cross-section how a lacunar fractal set of dimension smaller than 2 (Euclidean measure), we can write:

$$\sigma_0 = \sigma_0^* \, b^{-d_\sigma} \tag{2.15}$$

where σ_0^* is the fractal creep strength, which has the anomalous physical dimensions of $[F][L]^{-(2-d_\sigma)}$ and d_σ is the fractal dimension reduction.
Then, by replacing eq. (2.15) in eq. (2.14):

$$t_R = B_0 \left(\frac{\sigma_0}{\sigma}\right)^p = B_0 \left(\frac{\sigma_0^* \, b^{-d_\sigma}}{\sigma}\right)^p \tag{2.16}$$

and after some adjustments:

$$\sigma = \sigma_0^* \, b^{-d_\sigma} \, (B_0)^{\frac{1}{p}} (t_R)^{-\frac{1}{p}} \tag{2.17}$$

By taking logarithm of both sides:

$$\log \sigma = \log \sigma_0^* - d_\sigma \, \log b + \frac{1}{p} \log B_0 - \frac{1}{p} \log t_R \tag{2.18}$$

In eq. (2.18) the dependence of the rupture stress on the specimen size is pointed out, providing a reduction of the nominal applied stress for larger structures, for a given value of rupture time t_R.

Adopting the same concepts, for the generic stress rupture, we can write:

$$\sigma = \sigma^* b^{-d_\sigma} \tag{2.19}$$

Then, inserting eq. (2.15) and (2.19) in eq. (2.14), we can obtain the following fractal law for creep rupture:

$$t_R = B_0 \left(\frac{\sigma_0}{\sigma}\right)^p = B_0 \left(\frac{\sigma_0^* b^{-d_\sigma}}{\sigma^* b^{-d_\sigma}}\right)^p = B_0 \left(\frac{\sigma_0^*}{\sigma^*}\right)^p \tag{2.20}$$

Eq. (2.20) describes the fractal law for creep rupture, which is size-independent. As it can be seen, it is written in the same form of eq. (2.14), but in this case fractal creep properties are involved, instead of the corresponding nominal quantities.

On the other hand, we can suppose the same scaling effect on the creep threshold, we can write:

$$\sigma_{th} = \sigma_{th}^* b^{-d_\sigma} \tag{2.21}$$

Following this route, when the nominal creep strength σ is plotted against the rupture time t_R, a downward translation of the curves is expected due to the increasing specimen size, as schematically represented in fig. 2.3. The amount of the expected translation, described by Eq. (2.15), (2.19) and (2.21), it is independent on the stress level, but it depends on d_σ, which measure the disorder influence. As shown in fig. 2.3, the translation involves all the three regions, including the deviation branches, cause of the fractal quantities defined in Eq. (2.15) and (2.21).

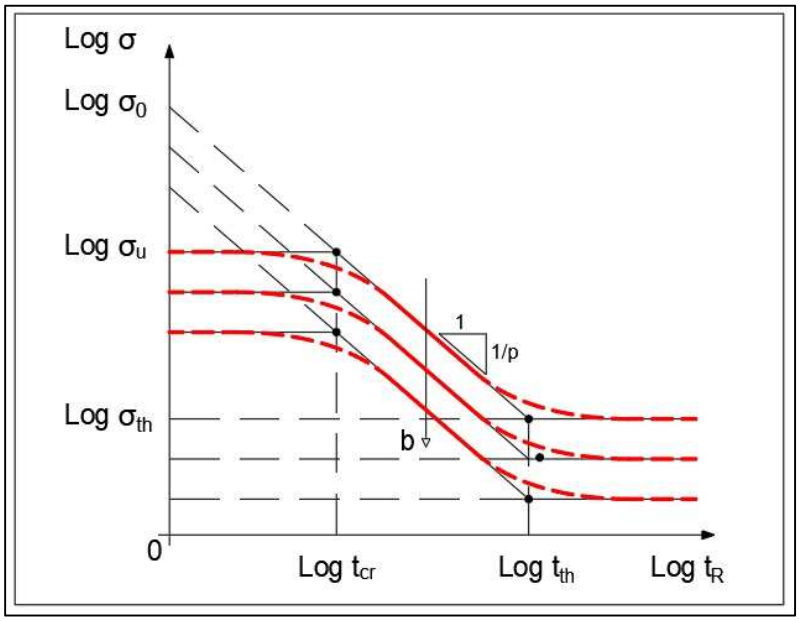

Figure 2.3 - Nominal diagram for creep rupture

Conversely, when fractal properties are considered, it is expected that all the data should collapse into a single curve, regardless of the specimen size (fig. 2.4).

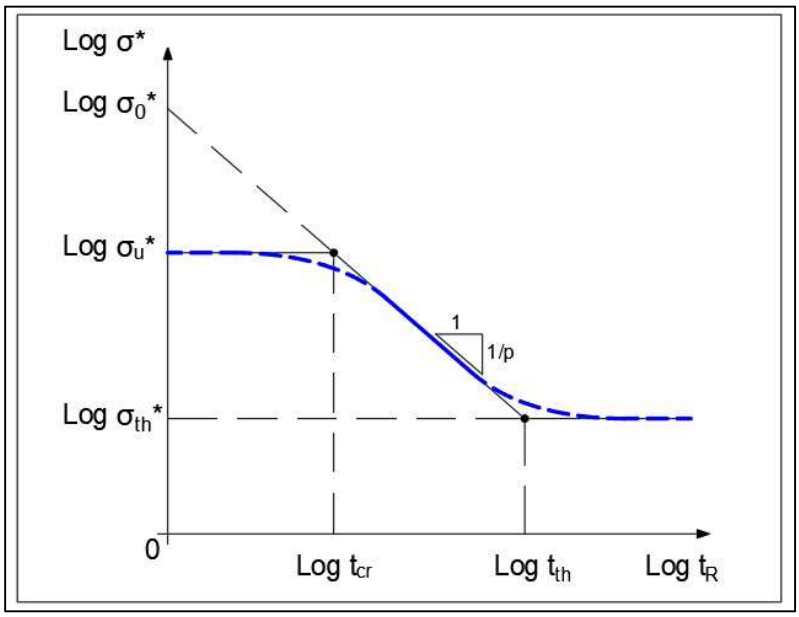

Figure 2.4 – Fractal diagram for creep rupture

As it can be seen, the procedure is in close agreement with that defined for fatigue in previous works. In this case the specimen life is described by the rupture time, which is not dimensionless if compared with the number of cycles to rupture. Nevertheless, by applying fractal geometry concepts, it has been shown that no complications occur.

2.4 Interpretation of crack-size effects on creep crack growth according to dimensional analysis

In this section, and the following, special attention will be given to the crack-size effects on creep crack growth, by means of dimensional analysis approach and fractal geometry concepts, adopting a similar procedure already used for specimen size effects.

As done for specimen size effects, our considerations will be based on previous experimental works reported in literature. In this context, the experimental work carried out by Tabuchi et al. [36] will be taken as benchmark. In order to study specimen size effect on creep crack growth rate, the authors conducted creep crack growth tests using CT specimens of various size.

More precisely, they used Standard CT specimens and ultra-large CT specimens, characterized by different width and thickness, reported in fig. 2.5. As it can be seen that, the specimen width is five times bigger for ultra-large specimens, while the thickness varies between 6.35 and 63.5 mm. It has to be noted that, by varying the specimen width of a scaling factor of five, also the initial crack length a_{in} scaled of the same ratio, keeping constant the ratio between a_{in} and W.

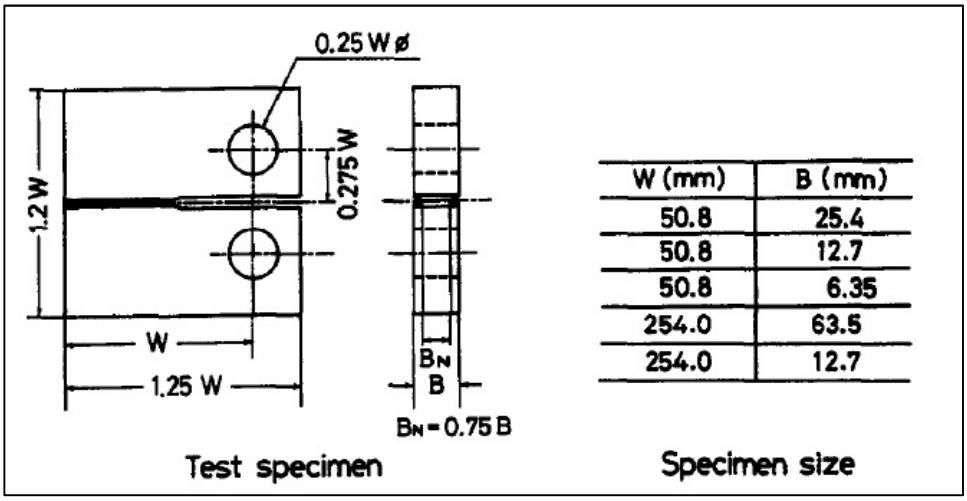

W (mm)	B (mm)
50.8	25.4
50.8	12.7
50.8	6.35
254.0	63.5
254.0	12.7

Figure 2.5 – Test specimens [36]

Carrying out creep tests, the authors attempted both the characterization of correlation creep crack growth rate (CCGR) in terms of the elastic stress intensity factor K and the C*-integral.

About da/dt-K correlation, experimental results are shown in fig. 2.6. As also reported in the paper, specimen thickness doesn't provide a clear effect on CGCR, when it is correlated with K. Conversely, a pronounced rightward translation of CCGR curves. The authors stated that for a given value of K, da/dt for ultra-large specimens was about 1000 times lower than that for standard specimens.

Since increasing specimen width implies larger crack length, this significant translation could be interpreted as a crack-size effect on creep crack growth, very similar to that observed for fatigue crack growth. In other words, this result lead to the assumption that shorter cracks have a faster propagation under creep conditions.

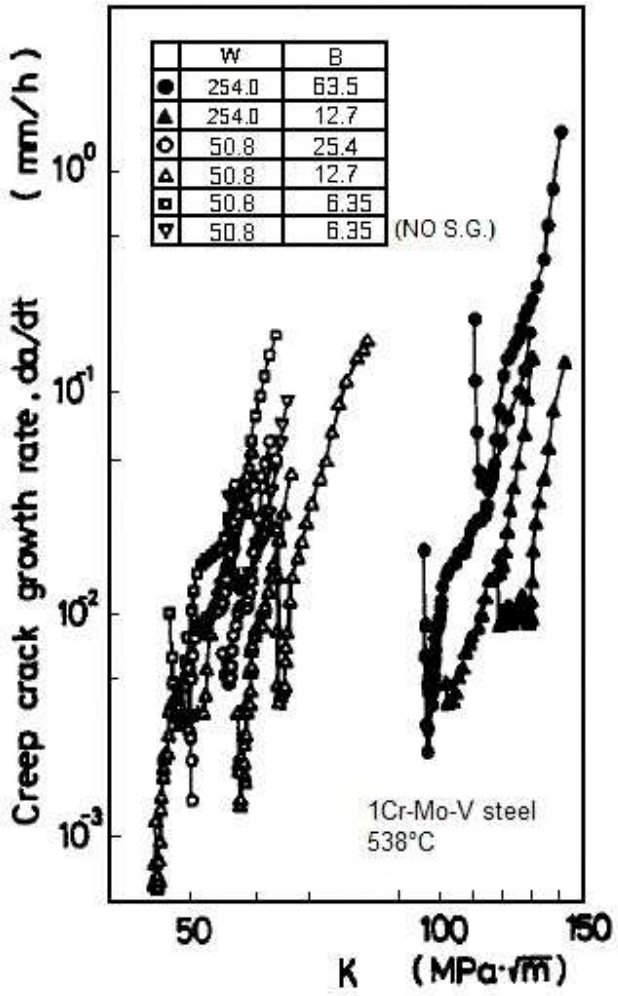

Figure 2.6 – d*a*/d*t*-*K* correlation reported in [36]

Considering the same tests, when CCGR is correlated with the *C**-integral as controlling parameter, conclusions are opposite. Looking at fig. 2.7, it can be noticed that specimen thickness has a noticeable effect, providing an increase of CCGR, for a given value of the controlling parameter. Strangely, the authors didn't notice any specimen width, or crack length, effect on CCGR, in contrast to

the correlation with K (fig. 2.6). This result appears curious, since the Ultra-large specimen width was five times larger than that related of standard CT- specimens.

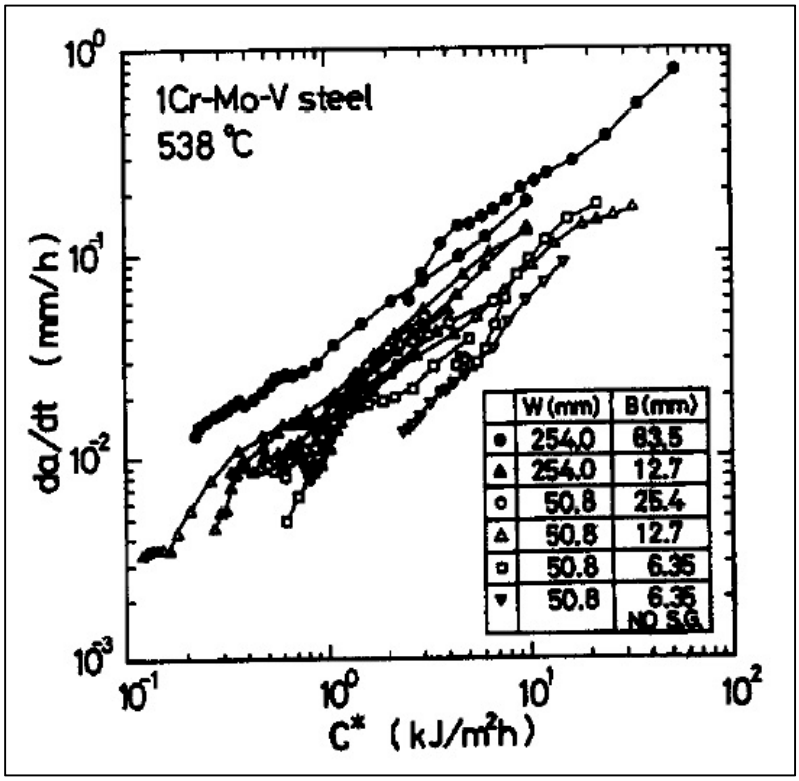

Figure 2.7 - da/dt-C* correlation reported in [36]

Later, these findings have been confirmed in other experimental works conducted by Tabuchi M. and Yagi K. in cooperation with Yokobori A.T. et al. [43] and Saxena [32].

Since in literature experimental results proving a counter-example are not founded, the existence of these effects, even if small, cannot be excluded.

In this section we will show that crack size effects on CCGR could be predictable, in the framework of dimensional analysis, even if they have not been

emphasised during the previous experimental campaigns. Again, two controlling parameters will be assumed, namely the elastic stress intensity factor *K* and the *C**-integral.

In the context of L.E.F.M., the following functional dependence can be stated:

$$\frac{\mathrm{d}a}{\mathrm{d}t} = \Phi\ (\sigma, K_I, T;\ \sigma_u, K_{IC}, K_{th}, \chi, T_M; a) \tag{2.22}$$

Physical dimensions of each parameter are already known, looking at tab. 2.1. In this case, as we said before, the scale effect under observation regards the crack length, instead of the specimen size considered for smooth specimens.

By applying Buckingham's Π Theorem ($\sigma_u, K_{IC}, \chi, T_M$ used as independent variables) we can obtain the following dimensionless relationship:

$$\frac{\mathrm{d}a}{\mathrm{d}t} = \left(\frac{\sigma_u}{K_{IC}}\right)^2 \chi\ \Phi_1\left(\frac{\sigma}{\sigma_u}, \frac{K_I}{K_{IC}}, \frac{K_{th}}{K_{IC}}, \frac{T}{T_M}, \left(\frac{\sigma_u}{K_{IC}}\right)^2 a\right) \tag{2.23}$$

The next step is assuming incomplete self similarity for certain dimensionless group. As results:

$$\frac{\mathrm{d}a}{\mathrm{d}t} = \chi\left(\frac{\sigma_u}{K_{IC}}\right)^2\ \Phi_2\left(\frac{\sigma}{\sigma_u}, \frac{K_{th}}{K_{IC}}, \frac{T}{T_M}\right)\left(\left(\frac{\sigma_u}{K_{IC}}\right)^2 a\right)^{\alpha_2}\left(\frac{K_I}{K_{IC}}\right)^{\alpha_1} \equiv C_0\ {K_I}^{\alpha_1} \tag{2.24}$$

where C_0 is a constant that depends on the crack length *a*.

As already discussed for smooth specimens, acting in the field of L.E.F.M., we find that scaling effects is governed by the characteristic length a_0, which can be considered a material property.

Following this route, we can tackle the pronounced decrease of CCGR related to Ultra-large CT specimens, observed when CCGR was correlated to the elastic stress intensity factor *K*. We will see in the next section that by means of fractal geometry concepts, more detailed considerations can be done about the translation of this curve, when Ultra-large specimens are tested.

On the other hand, repeating the same procedure for *C**-integral:

$$\frac{\mathrm{d}a}{\mathrm{d}t} = \Phi\ (C^*, T;\ \sigma_u, C_C^*, C_{th}^*, A, T_M; a) \tag{2.25}$$

The application of Buckingham's Π theorem provides:

$$\frac{\mathrm{d}a}{\mathrm{d}t} = \frac{C_C^*}{\sigma_u}\ \Phi_1\ \left(\ \frac{C^*}{C_C^*}\ , \frac{C_{th}^*}{C_C^*}\ , \frac{T}{T_M}\ , \frac{A{\sigma_u}^{n+1}}{C_C^*} a\ \right) \tag{2.26}$$

Again, the scale effect is governed by the same characteristic length defined, and previously discussed, for creep rupture.

Then, we have to apply incomplete self similarity for creep crack growth, on the basis of previous experimental work. As regard the parameter *C**, i.e. Π_1 dimensionless group, it has been reported from several authors as the controlling parameter for creep crack growth rate. As discussed in the previous section of this work, several experimental results lead to a power-law relationship between da/dt and *C**, with its exponent very close to 1. Furthermore, since the strong dependence on this parameter by crack growth, complete self-similarity cannot be assumed. So, the assumption of incomplete self-similarity in the Π_1 group, seems to be appropriate. About the dependence on the crack length, i.e. Π_4 dimensionless

group, not much can be said in according to previous work. As discussed before, researchers have not focused their attention about crack size effects on CCGR. In this sense, we put forward the assumption of incomplete self-similarity in Π_4, just supposing an analogy between creep and fatigue. We will see that dependence of CCGR on the crack length could be explained also in the framework of fractal geometry. Proceeding in this way, we can obtain:

$$\frac{\mathrm{d}a}{\mathrm{d}t} = \frac{C_C^*}{\sigma_u}\ \Phi_2\left(\frac{C_{th}^*}{C_C^*}, \frac{T}{T_M}\right)\left(\frac{A{\sigma_u}^{n+1}}{C_C^*}a\right)^{\alpha_2}\left(\frac{C^*}{C_C^*}\right)^{\alpha_1} \equiv D_0 {C^*}^{\alpha_1} \qquad (2.27)$$

Imposing $\alpha_1=\phi$, a perfect correspondence exists between eq. (2.27) and eq. (1.19), but in the latter case it is pointed out that D_0 depends on several parameters, including the crack length a.

2.5 Interpretation of crack-size effects on creep crack growth according to fractal geometry

A better interpretation of crack size effects on CCGR could be provided, when fractal crack-tip parameters are defined as controlling parameters.

Assuming K as controlling parameter for creep crack growth, let's start from the relationship involving nominal quantities:

$$\frac{\mathrm{d}a}{\mathrm{d}t} = C_0 {K_I}^m \qquad (2.28)$$

which is schematically respresented in fig. 2.8. In the figure is also represented the translation of these curves by varying crack length, consistently with experimental results previously discussed.

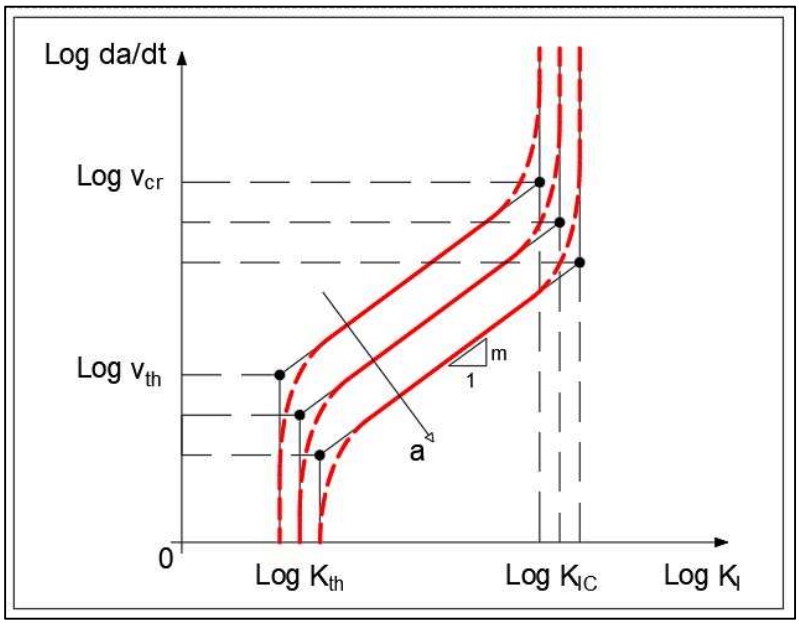

Figure 2.8 – Schematic representation of d*a*/d*t*-*K* diagram

Eq. (2.28) resembles the well-known Paris law defined for fatigue. Therefore, as done for fatigue by Carpinteri et al. ([12], [13], [27]), the following power-law dependencies can be used:

$$K_I = K_I^* a^{d_G/2} \tag{2.29}$$

$$a^* \simeq a^{1+d_G} \tag{2.30}$$

obtaining the following fractal law for creep crack propagation:

$$\frac{\mathrm{d}a^*}{\mathrm{d}t} = C_0^* \, K_I^{*m} \tag{2.31}$$

where:

$$C_0^* = (1 + d_G) \, C_0 \, a^{d_G(1+m/2)} \tag{2.32}$$

Inverting eq. (2.32), the nominal constant C_0 can be expressed as follow:

$$C_0 = \frac{C_0^*}{(1 + d_G)} a^{-d_G(1+m/2)} \tag{2.33}$$

pointing out the negative scaling on the crack length.

In close agreement to what done for fatigue, the existence of several fractal quantities is put forward, regarding some key points describing the CCGR curve in fig. 2.8. More precisely, the fractal fatigue threshold is introduced:

$$K_{th} = K_{th}^* \, a^{d_G/2} \tag{2.34}$$

Analogous considerations about fractal speed propagation, v_{th}^* and v_{cr}^* , lead to the following power law relationship:

$$v_{th} = \frac{v_{th}^*}{1 + d_G} a^{-d_G} \tag{2.35}$$

$$v_{cr} = \frac{v_{cr}^*}{1 + d_G} a^{-d_G} \tag{2.36}$$

Scaling laws described in eq. (2.35) and (2.36) are obtained by analogy of a generic speed propagation, starting from eq. (2.30) and by applying a chain derivation rule.

As for smooth specimens, creep crack growth curves are represented in a fractal referring system in fig. 2.9. When fractal quantities are involved, it is expected that all data should collapse into a single curve, crack-size independent.

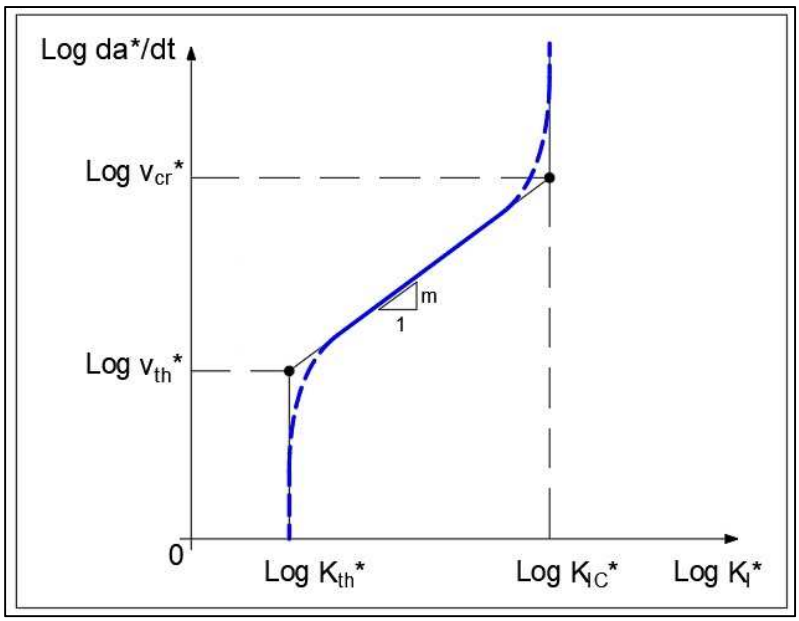

Figure 2.9 – Schematic representation of d*a*/d*t*-*K** diagram

As already noticed by applying dimensional analysis approach, when creep phenomenon is discussed in the framework of L.E.F.M., theoretical result is in close agreement with that achieved for fatigue. This is confirmed also when fractal concepts are used, for predicting creep crack growth rate.

As said before, the Renormalization Group Theory has been applied in solid mechanics, in the context of Linear Elastic Fracture Mechanics. An extension of these concepts to nonlinear fracture mechanics, is now provided. More precisely, for T.D.F.M. the existence of the fractal C*-integral will be putted forward, taking into account the dependence of C* by the crack length.

Then, considering the work U* dissipated during creep rupture, per unit time, as a macroscopic parameter, a straightforward application of the Renormalization Group Theory lead to:

$$U^* = C_0^* A_0 = C_1^* A_1 = \cdots = C_n^* A_n = \cdots = C_\infty^* A_\infty \tag{2.37}$$

where the first scale of observation could be the macroscopic one, with $C_0^* A_0 = C_C^* A$, A being the cross-sectional area, and the asymptotic scale of observation could be the microscopic one, with $C_\infty^* A_\infty = C^{**} A^*$, A^* being the measure of the fractal set representing the irregular fracture surface. Following this route, the renormalized C^*-integral has been introduced, C^{**}, with anomalous physical dimensions $[\mathrm{F}][\mathrm{L}]^{-(1+\mathrm{d}_G)}$. By some calculations, considering a through-thickness cracked body, the following power law relationship can be obtained:

$$C^* = C^{**} a^{d_G} \tag{2.38}$$

The crack size dependence of C^* is the same obtained in the elastic case for the nominal fracture energy $\mathcal{G}_F$.

As in the previous case, starting from the relationship including nominal quantities:

$$\frac{\mathrm{d}a}{\mathrm{d}t} = D_0 C^{*\phi} \tag{2.39}$$

And by using the following power-law dependencies:

$$C^* = C^{**} a^{d_G} \tag{2.40}$$

$$a^* \simeq a^{1+d_G} \tag{2.41}$$

we can obtain the following fractal law for creep crack propagation:

$$\frac{\mathrm{d}a^*}{\mathrm{d}t} = D_0^* \, C^{**\phi} \tag{2.42}$$

where:

$$D_0^* = (1 + d_G) D_0 a^{d_G(1+\phi)} \tag{2.43}$$

Inverting eq. (2.43), the nominal constant D_0 can be expressed as follow:

$$D_0 = \frac{D_0^*}{(1 + d_G)} a^{-d_G(1+\phi)} \tag{2.44}$$

pointing out the negative scaling on the crack length. In close agreement to what done for fatigue, the existence of the fractal C^* threshold is put forward:

$$C_{th}^{*} = C_{th}^{**}\, a^{d_G} \tag{2.45}$$

Exploiting fractal speed propagation, v_{th}^{*} and v_{cr}^{*}, defined in Eq. (2.35) and (2.36), again a translation of CCGR curves can be tacked, if represented in the nominal referring system, as in fig. 2.10.

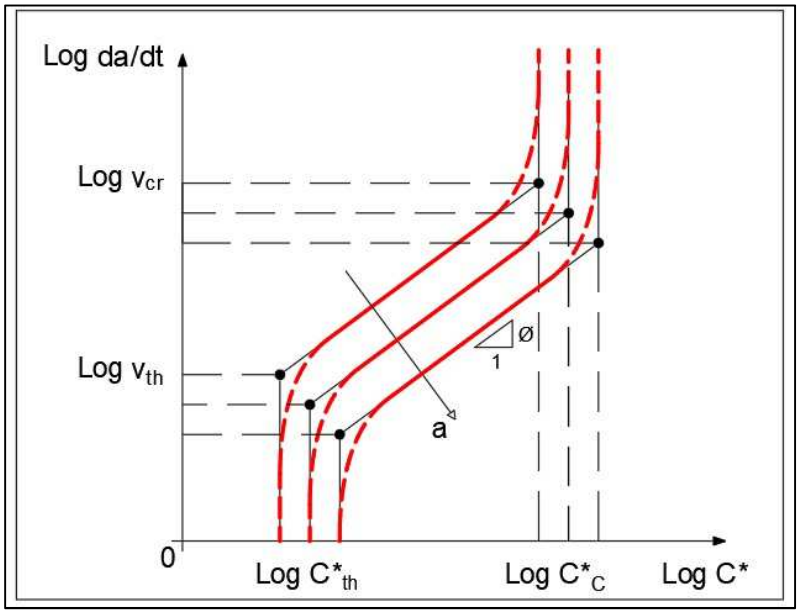

Figure 2.10 – Schematic representation of d*a*/d*t*-*C** diagram

Conversely, when renormalized quantities are involved, it is expected that all data should collapse upon a crack-size independent curve.

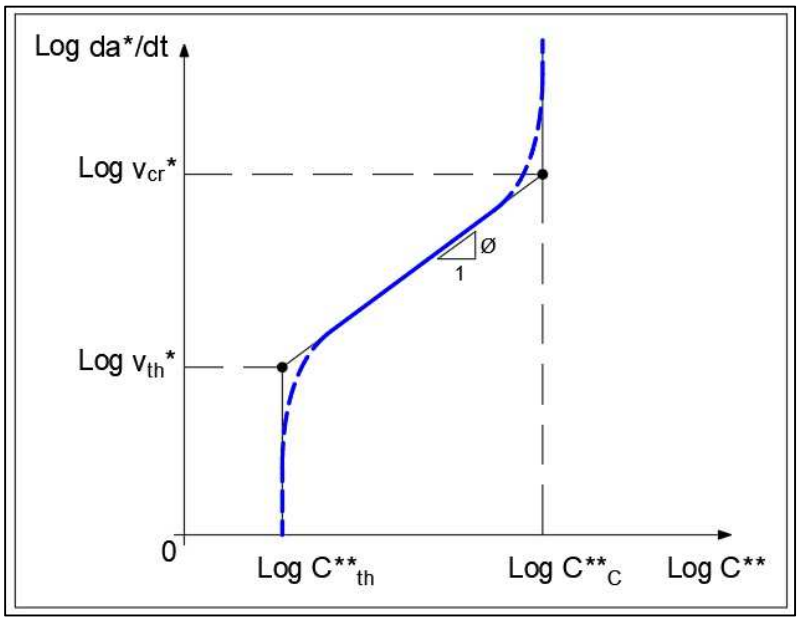

Figure 2.11 - Schematic representation of d*a*/d*t*-*C*** diagram

Therefore, also in the context of T.D.F.M, crack size effects find a theoretical reason, even if they seem not clear by previous experimental tests. Hence, it seems worthwhile to carry out other creep crack growth tests, exploring a wide range of specimen sizes, paying special attention to these effects, unclear until now.

2.6 Concluding remarks

In this final section, intriguing effects and implications that nonlinearity and disorder have on the stress field in the tip region of a cracked body, will be highlighted. On the basis of the previous discussion, the stress field at the crack-tip, presented in the introductive part within the framework of Fracture Mechanics, is referred to herein below for convenience:

$$\sigma_{ij} = K\, r^{-\frac{1}{2}}\, \widetilde{\sigma_{ij}}(\theta) \qquad (2.46.\text{a})$$

$$\sigma_{ij} = \left(\frac{J}{A_0 I_n}\right)^{\frac{1}{n_0+1}} r^{-\frac{1}{n_0+1}}\, \widetilde{\sigma_{ij}}(\theta) \qquad (2.46.\text{b})$$

$$\sigma_{ij} = \left(\frac{C^*}{A I_n}\right)^{\frac{1}{n+1}} r^{-\frac{1}{n+1}}\, \widetilde{\sigma_{ij}}(\theta) \qquad (2.46.\text{c})$$

Comparing eq. (2.46.a), (2.46.b) and (2.46.c), it is shown that the order of magnitude of the stress field is uniquely described by a crack-tip parameter, which is *K* for L.E.F.M, *J* for E.P.F.M., *C** for T.D.F.M. A stress singularity at the crack-tip always occurs, but in the last two cases, generally nonlinear fracture mechanics, it is weaker than for L.E.F.M. It can vary between ½ and 0, accordingly to the exponent n_0 and n, which describe the appropriate constitutive law. In order to prevent confusion, we called n_0 the hardening exponent in E.P.F.M., while in T.D.F.M. the exponent n relates to the creep stress sensitivity of the material (Norton's law).

Looking at eq. (2.46.b) and (2.46.c), the stress-field can be expressed in the same form of eq. (2.46.a), valid for the elastic case. In fact, if we define the following generalized stress intensity factors:

$$\overline{K}_P = \left(\frac{J}{A_0 I_n}\right)^{\frac{1}{n_0+1}} \qquad (2.47)$$

$$\overline{K}_C = \left(\frac{C^*}{A I_n}\right)^{\frac{1}{n+1}} \qquad (2.48)$$

the stress field at the crack-tip can be defined inserting eq. (2.47) and (2.48), respectively in eq. (2.46.b) and (2.46.c). Then, we obtain:

$$\sigma_{ij} = \overline{K}_P \, r^{-\frac{1}{n_0+1}} \, \widetilde{\sigma_{ij}}(\theta) \qquad (2.49.\text{a})$$

$$\sigma_{ij} = \overline{K}_C \, r^{-\frac{1}{n+1}} \, \widetilde{\sigma_{ij}}(\theta) \qquad (2.49.\text{b})$$

It has to be noticed that the generalized "plastic" S.I.F $\overline{K}_P$, and the generalized S.I.F. for creep $\overline{K}_C$, have anomalous physical dimensions, depending upon n_0 and n. More precisely:

$$[\overline{\mathrm{K}}_{\mathrm{P}}] = [\mathrm{F}][\mathrm{L}]^{-\frac{2n_0+1}{n_0+1}} \qquad (2.50.\text{a})$$

$$[\overline{\mathrm{K}}_{\mathrm{C}}] = [\mathrm{F}][\mathrm{L}]^{-\frac{2n+1}{n+1}} \qquad (2.50.\text{b})$$

It is interested that, also for creep, the respective controlling parameter $\overline{K}_C$ doesn't contain time in its physical dimensions, contrary to *C**-integral. Furthermore, $\overline{K}_C$ has the same physical dimensions of $\overline{K}_P$ when n_0 and n have the same value, although the different physical meaning of the exponents. This lead to the observation that, in the framework of fracture mechanics, creep phenomenon can be studied as a generic nonlinear problem.

Focusing on creep mechanism, and considering the two limit cases:

$$\text{For } n = 1 \qquad \rightarrow \qquad [\overline{\mathrm{K}}_{\mathrm{C}}] = [\mathrm{F}][\mathrm{L}]^{-\frac{3}{2}} \qquad (2.51.\text{a})$$

$$\text{For } n \to \infty \quad \rightarrow \quad [\overline{K}_C] = [F][L]^{-2} \tag{2.51.b}$$

When n=1 (linear case), the generalized stress intensity factor assumes its classical physical dimensions $[F][L]^{-3/2}$. Stress concentration around the crack tip occurs, since stress singularity is equal to 1/2. On the other hand, increasing n, i.e. increasing creep stress sensitivity, the generalized S.I.F. tends to assume the physical dimensions of a stress $[F][L]^{-2}$. Under these circumstances, also the stress singularity tends to disappear, implying an almost constant stress distribution near the crack-tip. In conclusion, as already noticed by Carpinteri [4] for power-hardening material, also for creep a transition from creep crack propagation (brittle) to plastic flow (ductile) collapse is evident, when material nonlinearity increases. Particularly, when $n \to \infty$, it seems that the model cannot predict another crisis different from the plastic collapse.

In this perspective, this conclusion is in close agreement with experimental results previously discussed. In the first part, we said that several authors founded that the suitable controlling parameter must be defined in according to creep ductility conditions.

Extending fractal concepts to nonlinear fracture mechanics, both E.P.F.M. and T.D.F.M., we can write:

$$J = J^* a^{d_G} \tag{2.52}$$

$$C^* = C^{**} a^{d_G} \tag{2.53}$$

where J^* and C^{**} are the fractal controlling parameters, defined respectively for E.P.F.M. and T.D.F.M.

Inserting eq. (2.52) and (2.53), in eq. (2.47) and (2.48) respectively, we can write:

$$\bar{K}_P = \left(\frac{J^* a^{d_G}}{A_0 I_n}\right)^{\frac{1}{n_0+1}} = \left(\frac{J^*}{A_0 I_n}\right)^{\frac{1}{n_0+1}} a^{\frac{d_G}{n_0+1}} = \bar{K}_P^* \, a^{\frac{d_G}{n_0+1}} \tag{2.54}$$

$$\bar{K}_C = \left(\frac{C^{**} a^{d_G}}{A I_n}\right)^{\frac{1}{n+1}} = \left(\frac{C^{**}}{A I_n}\right)^{\frac{1}{n+1}} a^{\frac{d_G}{n+1}} = \bar{K}_C^* \, a^{\frac{d_G}{n+1}} \tag{2.55}$$

Eq. (2.54) and (2.55) describe the power-law dependence of the nominal generalized stress intensity factors, on the crack length a. It is interesting to note that, for nonlinear fracture mechanics, the crack-size dependence is described both by d_G, which is a measure of the microstructural disorder, and by n (n_0), which describes the material nonlinearity.

As it has done for L.E.F.M., in this work we introduce the fractal generalized stress intensity factors, both for E.P.F.M. and T.D.F.M., which are crack-size independent.

$$\bar{K}_P{}^* = \left(\frac{J^*}{A_0 I_n}\right)^{\frac{1}{n_0+1}} \tag{2.56}$$

$$\bar{K}_C{}^* = \left(\frac{C^{**}}{A I_n}\right)^{\frac{1}{n+1}} \tag{2.57}$$

with their anomalous physical dimensions:

$$\left[\overline{\mathrm{K}}_{\mathrm{P}}{}^{*}\right] = [\mathrm{F}][\mathrm{L}]^{-\frac{2n_0+1+d_G}{n_0+1}} \qquad (2.58.\,\mathrm{a})$$

$$\left[\overline{\mathrm{K}}_{\mathrm{C}}{}^{*}\right] = [\mathrm{F}][\mathrm{L}]^{-\frac{2n+1+d_G}{n+1}} \qquad (2.58.\,\mathrm{b})$$

In contrast to K^* defined for L.E.F.M., for nonlinear fracture mechanics (E.P.F.M. and T.D.F.M.) physical dimensions of $\overline{K}_P{}^{*}$ and $\overline{K}_C{}^{*}$ depend upon d_G and the material nonlinearity, described respectively by the exponents n_0 and n.

As previously done by Carpinteri and Chiaia [8] in the context of L.E.F.M., a generalization of the stress field at the crack-tip can be provided as follows for E.P.F.M. and T.D.F.M.:

$$\sigma_{ij} = \overline{K}_P{}^{*}\, r^{-\frac{1-d_G}{n_0+1}}\, \widetilde{\sigma}_{\mathrm{ij}}(\theta) \qquad (2.59.\,\mathrm{a})$$

$$\sigma_{ij} = \overline{K}_C{}^{*}\, r^{-\frac{1-d_G}{n+1}}\, \widetilde{\sigma}_{\mathrm{ij}}(\theta) \qquad (2.59.\,\mathrm{b})$$

With eq. (2.59.a) and (2.59.b) a very important generalization is obtained, since they can describe the stress field at the crack-tip in the most general condition, considering a nonlinear (power-law hardening) material, which is also disordered. Fractal nonlinear crack-tip parameters are used, in order to consider both nonlinearity and disorder. Consequently, an attenuation of the stress singularity at the crack-tip is noticed, affected by n_0 (n) and d_G.

Focusing on creep, and considering that n generally varies between 1 and ∞, d_G between 0 and 1, the following limit cases can be identified:

$$\text{For } n = 1 \quad \Rightarrow \quad \left[\overline{\mathrm{K}}_{\mathrm{C}}{}^{*}\right] = [\mathrm{F}][\mathrm{L}]^{-\frac{3+d_G}{2}}; \quad \sigma_{\mathrm{ij}} \,\alpha\, r^{-\frac{1-d_G}{2}} \qquad (2.60.\mathrm{a})$$

$$\text{For } n \to \infty \quad \Rightarrow \quad \left[\overline{\mathrm{K}}_{\mathrm{C}}{}^{*}\right] = [\mathrm{F}][\mathrm{L}]^{-2}; \quad \sigma_{\mathrm{ij}} \,\alpha\, r^{0} \qquad (2.60.\mathrm{b})$$

$$\text{For } d_G = 0 \quad \Rightarrow \quad \left[\overline{\mathrm{K}}_{\mathrm{C}}{}^{*}\right] = [\mathrm{F}][\mathrm{L}]^{-\frac{2n+1}{n+1}}; \quad \sigma_{\mathrm{ij}} \,\alpha\, r^{-\frac{1}{n+1}} \qquad (2.60.\mathrm{c})$$

$$\text{For } d_G = 1 \quad \Rightarrow \quad \left[\overline{\mathrm{K}}_{\mathrm{C}}{}^{*}\right] = [\mathrm{F}][\mathrm{L}]^{-2}; \quad \sigma_{\mathrm{ij}} \,\alpha\, r^{0} \qquad (2.60.\mathrm{d})$$

When *n*=1, and no restrictions are imposed about d_G, the same result achieved by Carpinteri and Chiaia [8] is obtained, which emphasises only the influence of $\mathrm{d_G}$ (eq. 2.60.a). Conversely, when $n \to \infty$, we find the limit situation previously discussed for highly nonlinear materials, with the stress field predicting a ductile (plastic flow) collapse. Considering the variation of d_G, when it tends to vanish, the stress field is described as for the case of a generic power-law hardening material. In this case, only the nonlinearity material affects the stress field, with no influence of disorder. When d_G approaches the unity, giving evidence of the extreme disorder of the material, again the fractal generalized S.I.F. for creep assumes the physical dimensions of a stress, and the stress singularity disappears. Shortly, the result is equivalent to that obtained for highly nonlinear materials ($n \to \infty$,), when nominal quantities were employed.

Concluding, we can say that highly nonlinearity or extreme disorder play a main role in the definition of the stress field near the crack-tip, and then in the description of the kind of collapse. More precisely, when nonlinearity, or similarly the disorder, approach their upper bound values, the ductile collapse seems to be

the unique failure predictable. This is the same limit condition that occurs when sufficient small specimens are tested.

From this standpoint, a more extensive interpretation of experimental results previously mentioned, can be provided. This remark agrees with the fact that several authors, found a very good correlation of CCGR with the net section stress, as previously described, for very ductile creep materials.

An important question remains still open: What is the actual contribution of material nonlinearity and material disorder providing the resulting ductile collapse? At the moment, it seems that there is no way to answer, although some theoretical evidences have been pointed out in this section.

It could be interesting carry out specific experimental tests providing a better understanding of size effects related for creep mechanics, both on smooth specimens and cracked specimens. Testing specimens of different size, for instance ranging one order of magnitude in the characteristic dimension, could be sufficient to confirm the theoretical results stressed in this work. In addition, experimental campaign could emphasise the transition from a brittle to a ductile collapse, decreasing structural size with geometrical similitude. Although, at the moment, it seems not clear the effective contribution of nonlinearity and disorder providing the ductile collapse.

REFERENCES

[1] Basquin O.H. (1910) The exponential law of endurance tests. *Proceedings ASTM*, 10, 625-630.

[2] Barenblatt G.I. (1996) *Scaling, Self-similarity and Intermediate Asymptotics*. Cambridge: Cambridge University Press.

[3] Carpinteri A. (1981) "Size effect in fracture toughness testing: A dimensional analysis approach". In *Analytical and Experimental Fracture Mechanics* (Proceedings of an International Conference, Roma, Italy, 1980), Eds. G.C. Sih, M. Mirabile, Sijthoff & Noordhoff, Alphen an den Rijn, pp. 785-797.

[4] Carpinteri A. (1983) "Plastic flow collapse vs. separation collapse (fracture) in elastic-plastic strain-hardening structures". *Matèriaux et Constructions*, Vol. 16, No. 2, pp. 85-96.

[5] Carpinteri, A. (1994) "Fractal nature of material microstructure and size effects on apparent mechanical properties". *Mechanics of Matererials,* Vol. 18, pp. 89-101. Internal Report, Laboratory of Fracture Mechanics, Politecnico di Torino, N. 1/92, 1992.

[6] Carpinteri A. (1994) "Scaling laws and renormalization groups for strength and toughness of disordered materials". *International Journal of Solids and Structures*, Vol. 31, No. 3, pp. 291-302.

[7] Carpinteri A., Chiaia B. (1995) "Multifractal nature of concrete fracture surfaces and size effects on nominal fracture energy". *Materials & Structures*, Vol. 28, No. 8, pp. 435-443.

[8] Carpinteri A., Chiaia B. (1996) "Power scaling laws and dimensional transitions in solid mechanics". *Chaos, Solitons & Fractals*, Vol. 7, No. 9, pp. 1343-1364.

[9] Carpinteri A., Ferro G. (1994) "Size effects on tensile fracture properties: a unified explanation based on disorder and fractality of concrete microstructure". *Materials and structures*, Vol. 27, No. 10, pp. 563-571.

[10] Carpinteri A., Paggi M. (2007) "Self-similarity and crack growth instability in the correlation between the Paris' constants". *Engineering Fracture Mechanics*, Vol. 74, No. 7, pp. 1041-1053.

[11] Carpinteri A., Paggi M. (2009) "A unified interpretation of the power laws in fatigue and the analytical correlations between cyclic properties of engineering materials". International Journal of Fatigue, Vol. 31, No. 12, pp. 1524-1531.

[12] Carpinteri A., Paggi M. (2010) "A unified fractal approach for the interpretation of the anomalous scaling laws in fatigue and comparison with existing models". International Journal of Fracture, Vol. 161, No. 1, pp. 41-52.

[13] Carpinteri A., Paggi M. (2011) "Dimensional analysis and fractal modeling of fatigue crack growth". Journal of the ASTM International, Vol. 8, No. 10, pp. 1-13.

[14] Ciavarella M., Paggi M., Carpinteri A. (2008) "One, no one, and one hundred thousand crack propagation laws: a generalized Barenblatt and Botvina dimensional analysis approach to fatigue crack growth". Journal of the Mechanics and Physics of Solids, Vol. 56, No. 12, pp. 3416-3432.

[15] Garofalo, F. (1965) "*Fundamentals of creep and creep-rupture in metals*". Macmillan Series in materials science.

[16] Goldhoff R. (1963) "Stress concentration and size effects in a Cr-Mo-V steel at elevated temperatures". *Proceedings of the Institution of Mechanical Engineers,* Vol. 178, pp. 19-32.

[17] Harper M.P., Ellison E.G. (1977) "The use of C* parameter in predicting creep crack propagation rates". *Journal of Strain Analysis,* Vol. 12, No. 3, pp. 167-179.

[18] Harrison C.B., Sandor G.N. (1971) "High-Temperature crack growth in low-cycle fatigue". *Engineering Fracture Mechanics,* Vol. 3, pp. 403-420.

[19] Koterazawa R., Iwata Y. (1976) "Fracture mechanics and fractography of creep and fatigue crack propagation at elevated temperature". *Journal of Engineering Materials and Technology, Trans. of the ASME,* Vol. 98, No. 4, pp. 296-304.

[20] Koterazawa R., Mori T. (1977) "Applicability of fracture mechanics parameters to crack propagation under creep condition". *Journal of Engineering Materials and Technology, Trans. of the ASME*, Vol. 99, No. 4, pp. 298-305.

[21] Landes J.D., Begley J.A. (1976) "A fracture mechanics approach to creep crack growth". *ASTM Special Technical Publication* 590, pp. 128-148.

[22] Neate G.J. (1977) "Creep crack growth in 1/2% Cr – 1/2% Mo - 1/4% V steel at 565°C". *Engineering Fracture Mechanics*, Vol. 9, pp. 297-306.

[23] Nicholson R.D. (1976) "The effect of temperature on creep crack propagation in AISI 316 stainless steel". *Materials Science and Engineering,* Vol. 22, pp. 1-6.

[24] Nicholson R.D., Formby C.L. (1975) "The validity of various fracture mechanics methods at creep temperatures". *International Journal of Fracture*, Vol. 11, No. 4, pp. 595-604.

[25] Nikbin K.M., Webster G.A., Turner C.E. (1976) "Relevance of nonlinear fracture mechanics to creep cracking". *ASTM Special Technical Publication* 601, pp. 47-62.

[26] Nikbin K.M., Webster G.A., Turner C.E. (1977) "A comparison of methods of correlating creep crack growth". In: *Fracture*, Vol. 2 of the Proceedings of the 4th International Conference on Fracture (ICF4), 19-24 June 1977, Wterloo, Canada, 627-634.

[27] Paggi M., Carpinteri A. (2009) "Fractal and multifractal approaches for the analysis of crack-size dependent scaling laws in fatigue". Chaos, Solitons & Fractals, Vol. 40, No. 3 , pp. 1136-1145.

[28] Rice J.R. (1968) "A path independent and the approximate analysis of strain concentration by notches and cracks". *Journal of Applied Mechanics,* Vol. 35, pp. 379-386.

[29] Saxena A. (1980) "Evaluation of C* for the characterization of creep crack growth behaviour in 304 SS". *ASTM Special Technical Publication* 700, pp. 131-151.

[30] Saxena A. (1986) "Creep crack growth under non-steady-state conditions". *ASTM Special Technical Publication* 905, pp. 185-201.

[31] Saxena A., Ernst H.A., Landes J.D. (1983) "Creep crack growth behaviour in 316 SS at 594°C (1100° F)". *International Journal of Fracture,* Vol. 23, pp. 245-257.

[32] Saxena A., Yagi K., Tabuchi M. (1994) "Crack growth under small scale and transition creep conditions in creep-ductile materials". *ASTM Special Technical Publication* 1207, pp. 481-497.

[33] Siverns M.J., Price A.T. (1970) "Crack growth under creep conditions". *Nature,* Vol. 228, pp. 760-761.

[34] Siverns M.J., Price A.T. (1973) "Crack propagation under creep conditions in a quenched 2.25 chromium 1 molybdenum steel". *International Journal of Fracture,* Vol. 9, No. 2, pp. 199-207.

[35] Smith D.J., Webster G.A. (1981) "Characterizations of creep crack growth in 1 per cent Cr Mo V steel". *Journal of Strain Analysis,* Vol. 16, No. 2, pp. 137-143.

[36] Tabuchi M., Kubo K., Yagi K. (1991) "Effect of specimen size on creep crack growth rate using ultra-large CT specimens for 1 Cr-Mo-V steel". *Engineering Fracture Mechanics*, Vol. 40, pp. 311-321.

[37] Yokobori A.T., Yokobori T. (1989) "New concept to crack growth at high temperature creep and creep-fatigue". In: *Advances in Fracture Research*, Vol. 2 of the Proceedings of the 7th International Conference on Fracture (ICF7), 20-24 March 1989, Houston, Texas, 1723-1735.

[38] Yokobori A.T., Yokobori T., Kuriyama T., Kako T., Kaji Y. (1986) "Characterization of high temperature creep crack growth rate in terms of independent parameters". In: *Proceedings of the International Conference on Creep*, 14-18 April 1986, Tokyo, Japan, 135-140.

[39] Yokobori A.T., Yokobori T., Tomizawa H., Sakata H. (1983) "Parametric representation of crack growth rate under creep, fatigue and creep-fatigue interaction at high temperatures". *Journal of Engineering Materials and Technology,* Vol. 105, pp. 13-15.

[40] Yokobori T., Sakata H. (1979) "Studies on crack growth rate under high temperature creep, fatigue and creep-fatigue interaction – I. On the experimental studies on crack growth rate as affected by $\sqrt{a}\ \sigma_g$, σ_g and temperature". *Engineering Fracture Mechanics*, Vol. 13, pp. 509-522.

[41] Yokobori T., Sakata H. and Yokobori A.T. (1979) "Studies on crack growth rate under high temperature creep, fatigue and creep-fatigue interaction – II. On the role of fracture mechanics parameter $\sqrt{a}_{eff}\ \sigma_g$ ". *Engineering Fracture Mechanics*, Vol. 13, pp. 523-532.

[42] Yokobori T., Sakata H. and Yokobori A.T. (1979) "A new parameter for prediction of creep crack growth rate at high temperature". *Engineering Fracture Mechanics*, Vol. 13, pp. 533-539.

[43] Yokobori T., Tanaka T., Yagi K., Kitagawa M., Fuji A., Yokobori A.T., Tabuchi M. (1992) " Results of an intercomparison of creep crack growth tests made in Japan". *Materials at High Temperatures*, Vol. 10, pp. 97-107.